POLITECNICO DI TORINO
Repository ISTITUZIONALE

Integrating high-resolution geoinformation with local knowledge enhances flood risk assessment: A case study from rural Niger

Original
Integrating high-resolution geoinformation with local knowledge enhances flood risk assessment: A case study from rural Niger / Tiepolo, M., Abraiz, M., Ibrahim Housseini, M., Baoua, O., Belcore, E., Cannella, G., Ganora, D., Marmolejo Gutiérrez, A., Piras, M., Saretto, F., Vesipa, R.. - In: NATURAL HAZARDS RESEARCH. - ISSN 2666-5921. - ELETTRONICO. - (2026), pp. 1-25. [10.1016/j.nhres.2026.09.001]

Availability:
This version is available at: 11583/3015094 since: 2026-09-02T12:00:04Z

Publisher:
Elsevier

Published
DOI:10.1016/j.nhres.2026.09.001

Terms of use:

This article is made available under terms and conditions as specified in the corresponding bibliographic description in the repository

Publisher copyright

(Article begins on next page)

26 October 2026

Journal Pre-proof

Integrating high-resolution geoinformation with local knowledge enhances flood risk assessment: A case study from rural Niger

Maurizio Tiepolo, Muhammad Abraiz, Mohamed Ibrahim Housseini, Ousmane Baoua, Elena Belcore, Giorgio Cannella, Daniele Ganora, Alejandro Marmolejo Gutierrez, Marco Piras, Francesco Saretto, Riccardo Vesipa

PII: S2666-5921(26)00081-8

DOI: https://doi.org/10.1016/j.nhres.2026.09.001

Reference: NHRES 361

To appear in: *Natural Hazards Research*

Received Date: 10 June 2026

Revised Date: 1 September 2026

Accepted Date: 1 September 2026

Please cite this article as: Tiepolo, M., Abraiz, M., Housseini, M.I., Baoua, O., Belcore, E., Cannella, G., Ganora, D., Gutierrez, A.M., Piras, M., Saretto, F., Vesipa, R., Integrating high-resolution geoinformation with local knowledge enhances flood risk assessment: A case study from rural Niger, *Natural Hazards Research*, https://doi.org/10.1016/j.nhres.2026.09.001.

This is a PDF of an article that has undergone enhancements after acceptance, such as the addition of a cover page and metadata, and formatting for readability. This version will undergo additional copyediting, typesetting and review before it is published in its final form. As such, this version is no longer the Accepted Manuscript, but it is not yet the definitive Version of Record; we are providing this early version to give early visibility of the article. Please note that Elsevier's sharing policy for the Published Journal Article applies to this version, see: https://www.elsevier.com/about/policies-and-standards/sharing#4-published-journal-article. Please also note that, during the production process, errors may be discovered which could affect the content, and all legal disclaimers that apply to the journal pertain.

© 2026 Publishing services by Elsevier B.V. on behalf of KeAi Communications Co. Ltd.

Journal Pre-proof

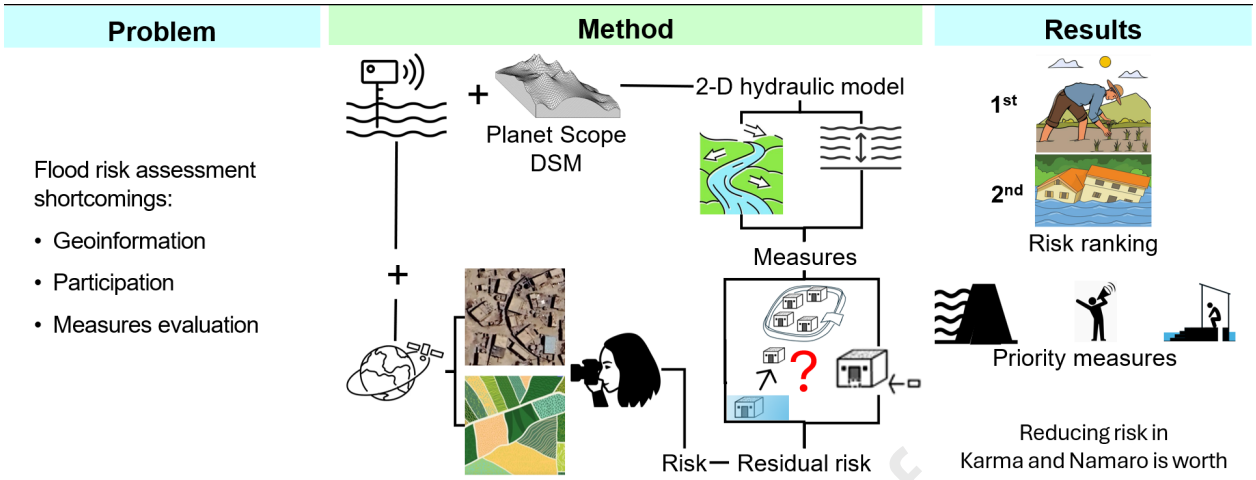

Journal Pre-proof

Journal Pre-proof

Integrating high-resolution geoinformation with local knowledge enhances flood risk assessment: A case study from rural Niger

Maurizio Tiepolo[1*], Muhammad Abraiz[2], Mohamed Ibrahim Housseini[3], Ousmane Baoua[4], Elena Belcore[2], Giorgio Cannella[1], Daniele Ganora[2], Alejandro Marmolejo Gutierrez[2], Marco Piras[2], Francesco Saretto[2], Riccardo Vesipa[2]

[1]Politecnico and University of Turin, Interuniversity Department of Regional and Urban Studies and Planning, viale Pier Andrea Mattioli 39, 10125 Turin, Italy
[2]Politecnico of Turin, Department of Environment, Land and Infrastructure Engineering, Corso Duca degli Abruzzi 24, 10129 Turin, Italy
[3]Université Abdou Moumouni de Niamey, Faculté d'Agronomie, BP 10896 Niamey, Niger
[4]Direction de la Météorologie Nationale du Niger, 08 rue du Grand hôtel, BP 218 Niamey, Niger

*Corresponding author, maurizio.tiepolo@polito.it

Abstract

Most flood risk assessments in rural areas of Low- and Middle-Income Countries rely on outdated, coarse-resolution geoinformation. Participation from exposed communities remains rare, and risk reduction measures are seldom identified. Our purpose is to address these shortcomings in a densely populated, frequently flooded rural area along the Niger River. The novelty of the study lies in the use of fine-grained spatial information and its integration with local knowledge, which led to the selection of appropriate risk-reduction measures. Risk was quantified monetarily as the product of hazard and expected damage. Riverine flooding and flash floods from tributaries are identified as the primary threats. Flood-prone areas for three return periods were identified using a 4-m resolution surface elevation model and BASEMENT's two-dimensional hydraulic modelling. Assets were first identified using Google Earth imagery and subsequently verified on-site. Risk reduction measures were initially selected through a participatory SWOT analysis and then prioritised using eight criteria. The study found that the areas under cultivation have remained stable over the last 10 years, but settlements significantly expanded in flood-prone areas. A centennial flood during the dry season could cause €5.4 million in damage, with the municipality of Kourteye accounting for €3.4 million. Risk was primarily determined by damage to irrigated crops rather than buildings. Priority measures included extending and reinforcing levees in rice-growing areas, providing an Early Warning System, and improving sanitation and hygiene. However, the benefits of reducing the risk outweigh the costs only in the municipalities of Karma and Namaro.

Keywords: BASEMENT; Cost-benefit; Digital Surface Model; Disaster risk reduction; Local knowledge; Risk management

1. Introduction

Ten years ago, the member states of the United Nations adopted the Sendai Framework for Disaster Risk Reduction 2015–2030 (SFDRR) in response to the increasing frequency of natural disasters [1]. This framework prioritised understanding disaster risk at the local level through pre-disaster assessments conducted in collaboration with at-risk communities [2]. Accordingly, the recommendations of grassroots organisations, activists [3], and scientists were embedded in its guiding principles, highlighting the urgency of local action [4–5], participation [6–8], and the incorporation of technical and local knowledge [9–10].

In the following decade, the United Nations Office for Disaster Risk Reduction published guidelines to support pre-disaster risk assessments. Among the most visible outcomes was the expansion of flood risk assessments (FRAs) in rural areas of Low- and Middle-Income Countries (LMCIs) [Table S1]. Researchers have developed FRAs using three main methods. The most widely used was the susceptibility analysis (11–14), which employed hazard and vulnerability indicators weighted using the Analytic Hierarchy Process, as defined by Saaty [15]. Hydraulic modelling, based on the work of Büchele et al. [16] and Apel et al. [17] and practised since the early 2010s [18–19], came second. Finally, the identification of flood-prone areas from Earth observations, based on the seminal work of Brivio et al. [20] and subsequently applied in various contexts [21], was less common.

These assessments used coarse, outdated geoinformation [22–23], limited field evidence [24], rarely followed a participatory process, and often overestimated risk levels [25]. Simultaneously, only a limited number of FRAs addressed risk evaluation [26–27], and those that did were confined to individual locations [28–31] or catchments [32–33]. Without addressing these limitations, FRAs remain inaccurate, standalone tools that fail to contribute to risk management.

This study aims to address persistent shortcomings in hazard identification, participation, and risk reduction strategies. The challenge raises a key research question: how can FRA refinements enhance risk management? To answer this question, we conducted a participatory, high-resolution assessment along a stretch of the Niger River located upstream of Niamey. The assessment addresses two distinct inundation mechanisms: fluvial flooding along the Niger River floodplain and pluvial flash flooding in the Karma Wadi, a Niger River sub-catchment. In this densely populated, semi-arid rural area exposed to catastrophic flooding, information was scarce, and insecurity constrained access to the terrain. Despite these limitations, we hypothesised that determining flood risk by integrating high-resolution geoinformation with local knowledge through a participatory process was not only feasible but also essential to identifying viable risk-reduction measures. In rural contexts in LMICs, the study's novelties lie in the granularity of the geoinformation considered and its integration with participatory methods across all FRA phases.

In collaboration with four local riverside governments, we identify flood-related threats, estimate risk levels through hydraulic flood modelling and field inspections, assess the contribution of minor tributaries to crop flooding, identify measures to reduce expected damage (ED), and estimate the associated costs and benefits. Together, these steps demonstrate how a detailed, participatory FRA can improve risk management at the mesoscale.

2. Methodology

2.1. Case study

The FRA was conducted in a rural region extending 450 km² along a 58 km stretch of the Niger River, upstream of Niamey. To avoid boundary effects in the hydraulic simulations, the modelled domain was extended approximately 10 km upstream and 20 km downstream of this reach, giving a total simulated length of about 90 km (see section 2.4.3.1). On the right bank, six wadis and the Dargol and Sirba Rivers flow intermittently into the Niger River, while the left bank features a hydrographic network comprising eleven wadis (Fig. 1).

The area has a hot, semi-arid climate, with a rainy season lasting from June to September. During this period, tributaries in the middle basin may generate local flooding. Conversely, rainfall in the upper Niger basin leads to the Guinean flood [34], which reaches the study area during the dry season from November to February. The territory between the two state roads running parallel to the Niger River has a population density of 160 inhabitants per km². It

includes four rural towns and 91 smaller settlements, 36 of which are situated on 13 islands. Administratively, it falls within the municipalities of Bitinkodji, Gothèye, Karma, Kourteye and Namaro. Approximately 72,000 inhabitants [35] sustain their livelihoods through horticulture, rice cultivation in large hydro-agricultural developments (AHA) and in traditional smaller fields, rain-fed millet (*Pennisetum glaucum*), often intercropped with cowpea (*Vigna unguiculata*) or groundnut (*Arachis hypogaea*), and livestock breeding.

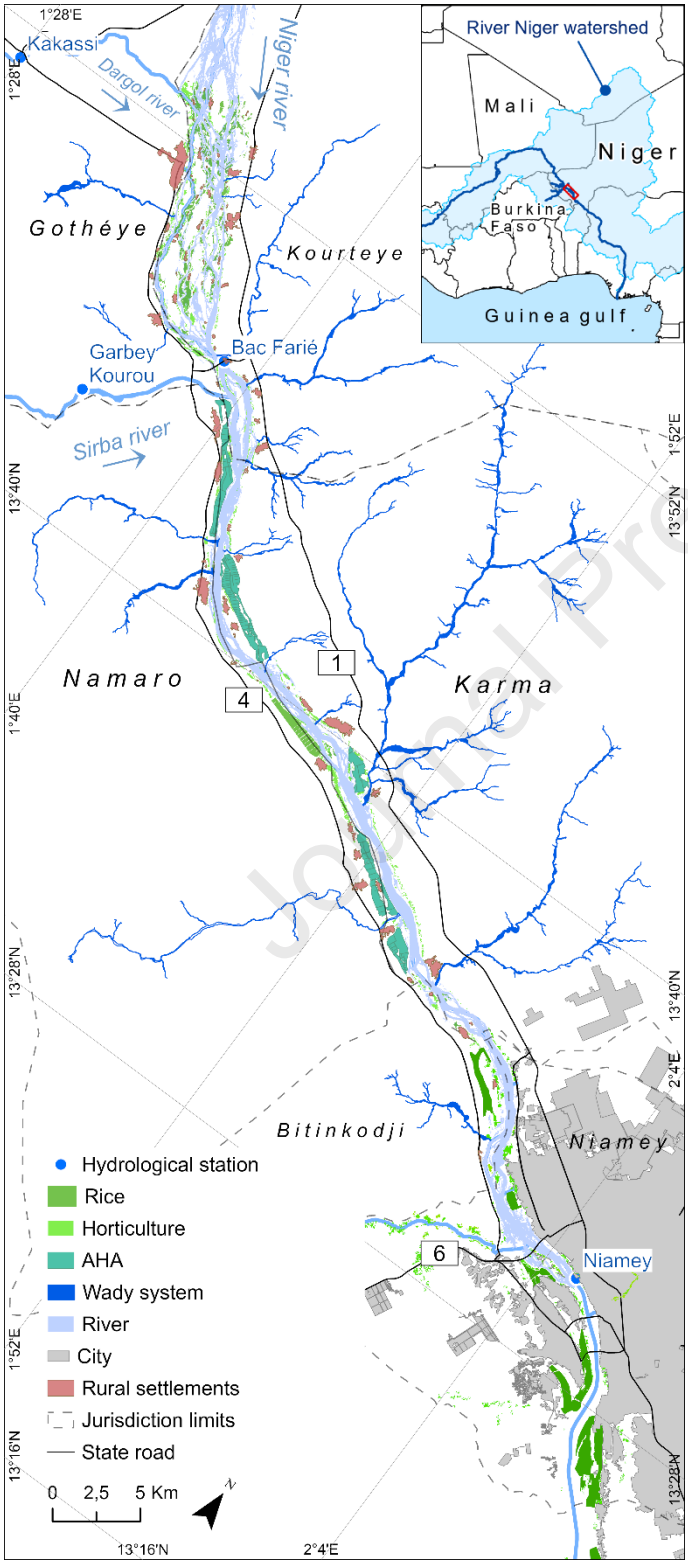

Fig. 1. Study area.

Journal Pre-proof

Based on these hydro-climatic and territorial conditions, the analysis considered two distinct flood-generating systems. The first is the Niger River itself, for which we assessed fluvial flooding along the main river corridor and its floodplain. Along the analysed reach, the active channel varies in width from about 0.6 to 3.5 km, with the widest sections occurring between the Dargol and Sirba confluences. In this sector, the river shows a braided morphology, with multiple active subchannels and numerous islands. Because of the seasonal hydrological regime described above, the fluvial analysis considered both local floods generated during the rainy season and the Guinean flood arriving from the upper basin during the dry season.

The second flood-generating system is the Karma Wadi, located on the left bank. Although the Karma area is already included in the broader fluvial flood assessment, the wadi was analysed separately for pluvial flash flooding because local partners identified it as recurrently causing damage during the rainy season. This process particularly affects the Koutoukalé hydro-agricultural development. The Karma Wadi basin considered for the pluvial analysis covers approximately 382 km², with a maximum flow length of about 36 km, a form factor of 0.295 and an average terrain slope of approximately 17%. These morphometric characteristics favour rapid runoff concentration during intense rainfall events, making the basin relevant for flash-flood analysis.

2.2. Conceptual framework

FRAs include risk identification, analysis and evaluation [36]. Here, the risk level is expressed in monetary terms as the product of hazard probability and expected damage (ED) [29, 37–39]. Risk analysis links hydrology, topography, hydraulic and damage modelling. Hydrology defines the probability and magnitude of the analysed flood scenarios and provides the return period (RP) specific hydrographs used as hydraulic boundary conditions. Topography provides a digital surface model (DSM), which serves as the spatial basis for hydraulic modelling. The hydraulic model transforms the hydrological and topographic inputs into maximum flood-depth rasters, from which flood extents are derived. ED and risk are then estimated from these hydraulic outputs. Risk evaluation includes participatory identification of risk-reduction measures, estimation of their potential impact, and cost-benefit analysis using a quantitative method [40] that integrates local and technical knowledge [41] (Fig. 2). The assessment is based on daily river discharge and rainfall data, DSM, satellite imagery, hydrological-hydraulic modelling, field visits, agricultural commodity prices and property values, the population census, the results of focus groups with the affected municipalities [42], and the findings of previous surveys on land reclamation and per capita healthcare expenditure (Table 1).

Journal Pre-proof

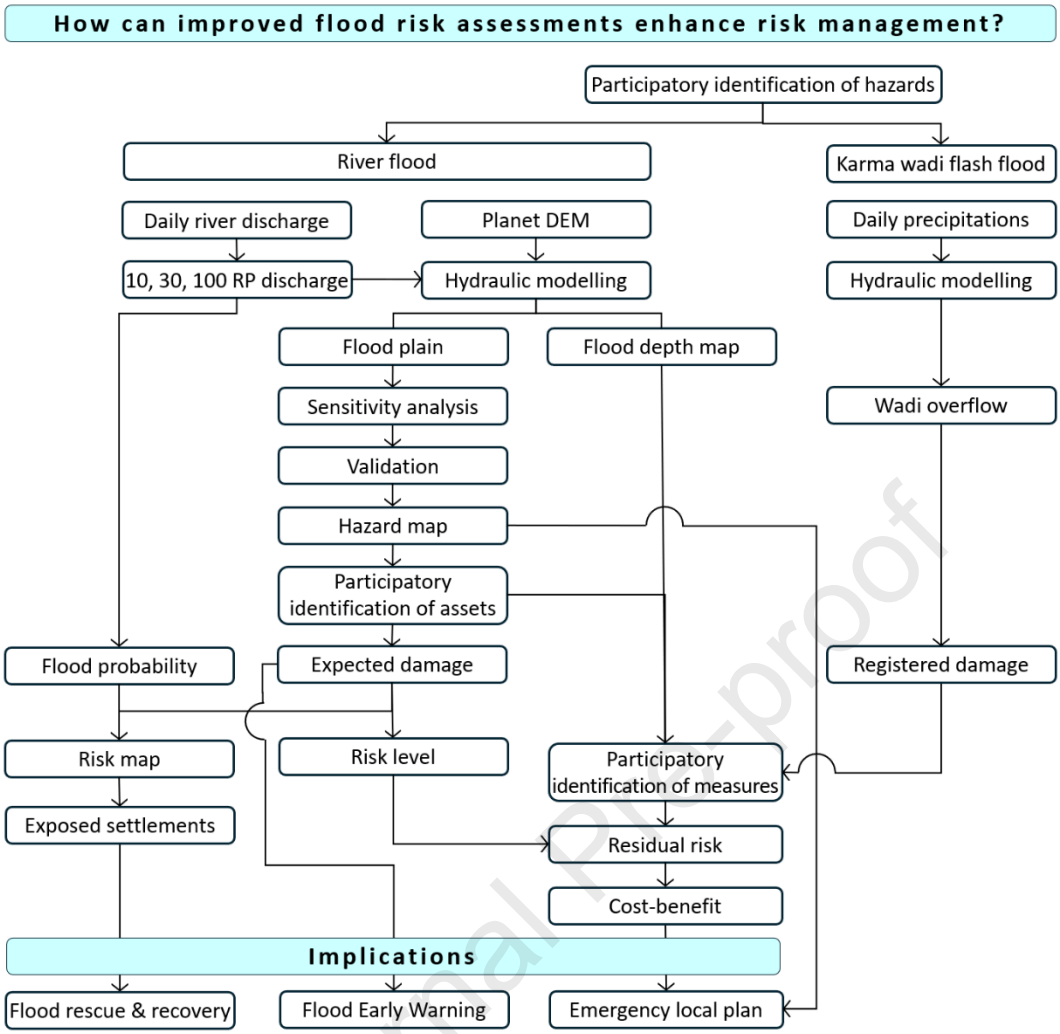

Fig. 2. Method flowchart.

Table 1
List of data and their source used in the FRA.

Data type	Source	Period	Output
River discharge	Hydrometers	1955–2024	Hazard
Daily precipitation	Karma climate ground station	1994–2024	
DSM	PlanetScope 4 m resolution	2019–2021	Damage
Flood edge	Flood numerical modelling	2025	
Flood validation	Sentinel-2	Aug. 2024, Feb. 2025	
DSM sensitivity	Drone 0.1 m on Touré site	2019	
Population	Population national census	2012	
Assets	Google Earth images	Jan. 2014, Feb. 2024	
	Field inspection on 24 sites	Feb. 2024	
	Information system rural markets	2024	
	Compensation for public works	2024	
Settlements names	Directory of human settlements	2012	
Measures identification	Focus group with municipalities	Sept. 2025	Risk evaluation
Measures selection	SWOT analysis	Sept. 2025	
Measures priority	Focus group with municipalities	Sept. 2025	
Measures costs	Municipalities, AHA managers	Sept. 2025	
Land recovery	Survey	2019	
Health benefits	Per capita health expenditure	2012–2023	

Journal Pre-proof

2.3. Risk identification

Risk identification was conducted on 30–31 October 2024 in the presence of mayors, rural extension services, environmental units, and early warning and emergency response systems, as well as representatives of farmers, livestock breeders, and women gardeners from the Karma and Namaro jurisdictions.

2.4. Risk analysis

We conducted risk analysis separately for the two flood-generating mechanisms identified in the study area: fluvial flooding along the Niger River and pluvial flash flooding in the Karma Wadi. For both mechanisms, the analysis followed the same sequence: hydrological estimation of return-period-specific hydrographs, two-dimensional hydraulic simulation of flood propagation and inundation, extraction of maximum flood-depth rasters and derived flood extents, estimation of expected damage to the exposed assets, and calculation of risk levels using the probability associated with each return period (RP).

2.4.1. Hydrological input

Hydrological inputs were estimated separately for the fluvial and pluvial scenarios and were used to generate the hydrographs imposed as inflow conditions in the hydraulic models.

2.4.1.1. Fluvial hazard. To analyse extreme flood events in the study area, we processed hydrological observations from the Kakassi (Dargol River), Garbey Kourou (Sirba River), and Niamey (Niger River) stations using the approach described by Tiepolo et al. [43]. Fig. 3 shows the temporal availability of the discharge records used at each station.

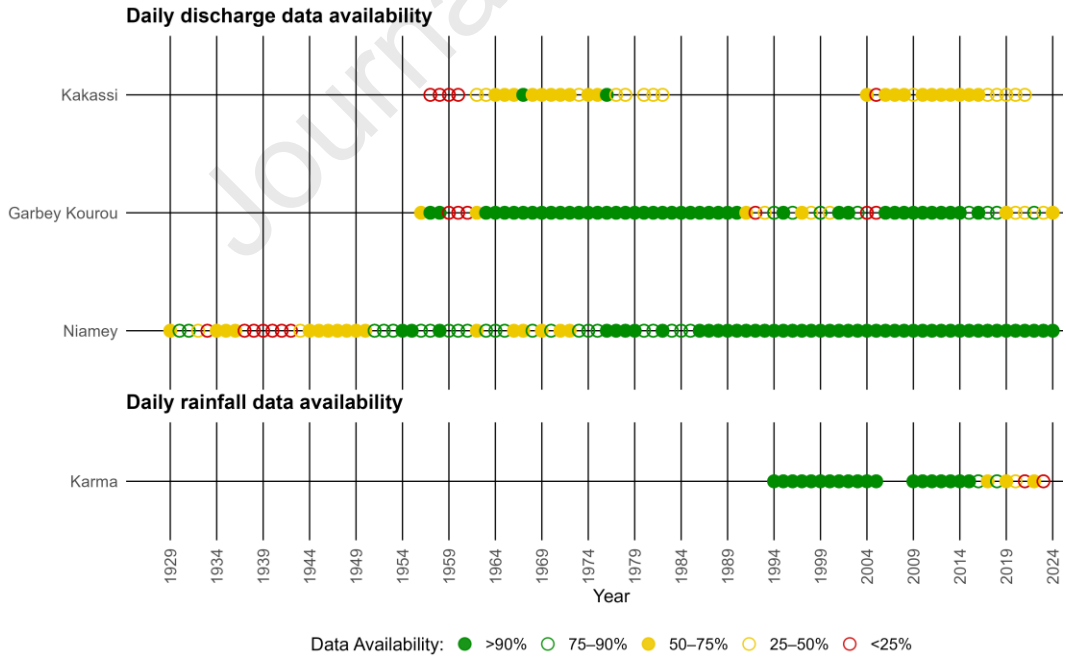

Fig. 3. Daily river discharge and daily rainfall data availability by station.

We fitted the resulting peak distributions to the generalised extreme value distribution using the L-moments method. For the data-limited Kakassi station, the Garbey Kourou distribution scaled by catchment area was applied after confirming homogeneity – hereby defined as basins having the same at-site frequency distribution except for a site-specific scale factor – between

the two basins through the test proposed by Hoskings and Wallis, giving results [44]: H_1 = 0.03, H_2 = 0.02, H_3 = 0.58. Extreme events for this station were then computed as:

$$Q^T_{Kakassi} = Q^T_{Garbey\ Kourou} * \alpha \quad (1)$$

where $\alpha = A_{Dargol\ basin}/A_{Sirba\ basin} = 0.186$.

Given the distinctive two-peak behaviour of the Niger River in Niamey [43], separate analyses were performed for the periods from June to October and from November to May. The section's input discharge was then calculated by solving the water balance equation:

$$Q^T_{Niamey} = Q_{Upstream,T} + Q^T_{Kakassi} + Q^T_{Garbey\ Kourou} \quad (2)$$

Rewriting Equation 1 for $Q_{Upstream,T}$, yields the following:

$$Q_{Upstream,T} = Q^T_{Niamey} - Q^T_{Garbey\ Kourou}(\alpha + 1) \quad (3)$$

In dry season, when $Q_{Garbey\ Kourou}$, $Q_{Kakassi} \approx 0$, this simplifies to:

$$Q_{Upstream,T} = Q^T_{Niamey} \quad (4)$$

The resulting discharges [Table S2] were used to construct the inflow hydrographs imposed at the upstream Niger River boundary and at the Sirba and Dargol tributary boundaries of the fluvial hydraulic model (Fig. 4a)

2.4.1.2. Pluvial hazard. The pluvial flash-flood analysis used observed daily rainfall data from 1994 to 2025 at the Karma station (Fig. 3). Unlike the fluvial analysis, this component required a rainfall–runoff transformation to estimate inflows generated by intense local rainfall over the Karma Wadi basin.

We collected extreme daily rainfall events using the metastatistical extreme value distribution [45]. We then computed hourly hyetographs using the Chicago method, parameterised to reflect typical local precipitation events. Infiltration loss was then represented using the Horton method with locally calibrated parameters [46], and runoff hydrographs were calculated using the instantaneous unit hydrograph method (Tables S3–S4).

Because of the topography of the Karma Wadi catchment and the location of the Koutoukalé AHA, the analysis was conducted separately for the two contributing sub-basins of stream 1 and stream 2 (Fig. 4b). The same RPs adopted for the fluvial hazard were considered, according to a fundamental principle of multi-hazard analysis [47]. We imposed the resulting runoff hydrographs as inflow boundary conditions in the pluvial hydraulic model for each RP.

Journal Pre-proof

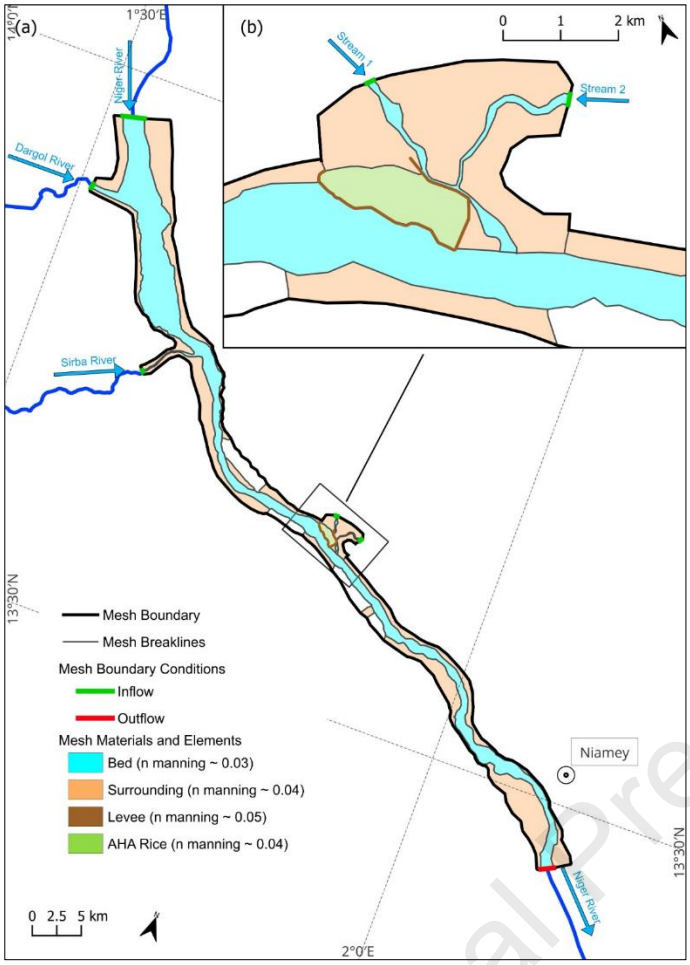

Fig. 4. Hydraulic model mesh (a) and the Karma Wadi that threatens the Koutoukalé AHA (b).

2.4.2. Topographic input

We used a 4 m-resolution digital surface model as the main topographic input for the hydraulic simulations. The DSM was created from 13 pairs of PlanetScope satellite images acquired between 2019 and 2021. Notably, PlanetScope imagery offers a spatial resolution of 3 m and a ground sampling distance of 3–4 m, with daily global coverage. We created the DSM using a sequential bi-stereo image-matching workflow implemented in ENVI's DSM extraction module. This workflow involved estimating regional elevation from image metadata, introducing ground control points from the Shuttle Radar Topography Mission (SRTM) global DEM, generating tie points and epipolar images, and computing stereo DSMs [48]. We then mosaicked and averaged the DSMs from each stereo pair to produce a seamless, high-spatial-resolution surface model over the Niger River and Karma Wadi domains (Fig. 5).

Journal Pre-proof

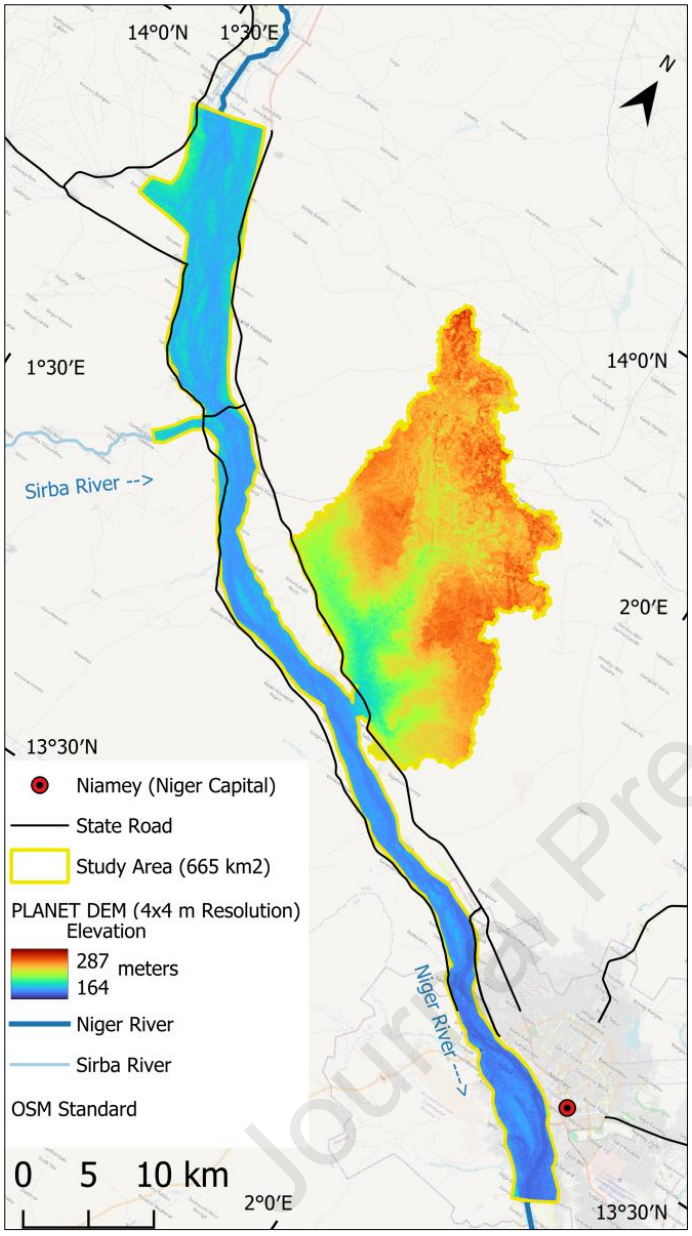

Fig. 5. PlanetScope-derived DSM with 4 m resolution created over the Niger River and the Karma Wadi basin.

2.4.3. Hydraulic modelling

Hydraulic simulations were performed using BASEMENT, a well-established and extensively benchmarked numerical modelling environment for solving the two-dimensional unsteady shallow-water equations. Its numerical robustness and computational efficiency have been assessed against a range of benchmark tests [49]. BASEMENT was selected for this study because it supports GPU-based parallel computation and integrates readily into an automated modelling workflow. We carried out pre- and post-processing in QGIS to leverage its GIS capabilities, while Python scripts automated model setup, execution, and data handling across different computational domains and return periods.

2.4.3.1. 2D Hydraulic simulations. BASEMENT simulated both fluvial and pluvial floods with its two-dimensional, unsteady shallow-water solver, using separate domains for the Niger River and Karma Wadi systems. The fluvial domain covered approximately 90 km of the Niger River, with model boundaries placed well outside the main risk area. The pluvial domain covered the Karma Wadi and its junction with the Niger River, focusing on the Koutoukalé AHA. Table 2

Journal Pre-proof

summarises all model parameters, boundary conditions, and numerical solver settings, along with their justification.

Table 2
Model parameters, boundary conditions and numerical solver settings

Parameter	Value	Observation
Mesh element area (max)	20 m²	Below DSM pixel area (16 m²)
Bed elevation	PlanetScope DSM, 4 m, with discharge correction (DCT)	Corrects for submerged riverbed [50] field bathymetry not feasible
Manning's n, riverbed	0.03	[51]
Manning's n, floodplain	0.04	[51]
Manning's n, wadi bed	0.03	[51]
Manning's n, floodplain/AHA	0.04	[51]
Manning's n, levee (pluvial)	0.05	[51]
Downstream boundary, fluvial	Fixed WSE = 183 m a.s.l., ~20 km downstream	Beyond influence of study reach
Downstream boundary, pluvial	WSE from separate Niger mean-discharge run	
Inflow boundary conditions	RP10/30/100 hydrographs: Niger, Sirba, Dargol; Karma Wadi sub-basins	See 2.4.1
Hydrograph duration, fluvial	4 days, centred on peak (±2 days)	Verified sufficient for depths to stabilize before extraction
CFL	0.9	Below stability limit (1.0)
Fluid density	1000 kg/m³	Fresh water
Maximum time step	100 s	Upper bound; actual step set by CFL
Minimum water depth	0.01 m	Wetting/drying threshold
Initial time step	0.02 s	Conservative start value
Minimum time step	0.0001 s	Floor for adaptive scheme near dry cells
Output raster	Maximum water depth, 4 m resolution	Inundation extent derived by thresholding (depth > 0)

Each domain used an unstructured triangular mesh built from breaklines, boundary-condition lines, and the PlanetScope DSM, with element area capped at 20 m² to avoid adding false precision beyond the DSM's 4 m (16 m² pixel) resolution. Breaklines marked domain edges, controlled mesh density, and separated roughness zones. In the fluvial model, hydrographs entered at the upstream Niger boundary and at the Sirba and Dargol tributaries, with a fixed downstream water level set about 20 km below the study reach so it would not affect upstream simulated flow. In the pluvial model, runoff hydrographs from the two Karma Wadi sub-basins entered at the stream inlets, while downstream water levels came from a separate Niger River simulation under average discharge.

We used the DSM to set bed elevations on the mesh. Because we used a DSM rather than a bare-earth DTM, and field bathymetry was not feasible for economic, logistical, and security reasons, we applied the discharge-correction method of Choné et al. [50] to the Niger River simulations to account for the submerged riverbed. This mattered less for the Karma Wadi, since its DSM was captured during a dry period in a semi-arid, sparsely vegetated area.

We assigned Manning roughness values by mapped surface type. In the fluvial domain: n=0.03 for the riverbed and n=0.04 for the surrounding floodplain. In the pluvial domain: n=0.03 for the wadi bed, n=0.04 for the surrounding floodplain and the rice-growing AHA cropland, and n=0.05 for the levee. These follow standard reference values from Chow [51]. Areas along the river protected by levees were left unmeshed and treated as no-flow zones, assuming they would not be reached by the Niger River flood. The Koutoukalé AHA, adjacent to the Karma Wadi, was the exception: here the concern is not the Niger flood but the pluvial flash flood arriving through the wadi, against which the levee provides only partial protection. This area, together with the levee, was therefore included in the mesh — with the crest elevation

added manually where the DSM did not represent it clearly — to assess the extent to which the AHA could still be inundated despite the levee.

The modelled reach extended for approximately 90 km along the Niger River, with the active channel width ranging from 0.6 to 3.5 km. A four-day inflow hydrograph, centred on the flood peak and covering the two days before and after the crest, was used to allow the flood wave to propagate through and exit the computational domain. The simulation duration was verified as sufficient for water depths within the domain to become unaffected by the initial conditions before extracting results for the hazard and risk analyses.

Simulations were run for the 10-, 30- and 100-year return periods on cloud-based virtual machines. The solver used BASEMENT's default settings for the explicit shallow-water scheme. Main outputs were maximum water-depth rasters and flood extents at 4 m resolution, matching the DSM, processed in QGIS for mapping and damage assessment.

2.4.3.2. Sensitivity analysis. A sensitivity analysis assessed how vertical uncertainty in the PlanetScope-derived DSM could affect simulated water depths. Because no high-resolution topographic benchmark was available within the Niger River reach, the analysis used auxiliary data from previous research [52] for the Touré settlement, located along the Sirba River approximately 34 km upstream of its confluence with the Niger River (Fig. 6a). The lower Sirba River lies in the same geomorphological and climatic setting as the study area, and both areas are covered by the same PlanetScope-derived DSM. A drone-derived DSM with 0.08 m horizontal resolution was available for a 1.8 km river reach at Touré and was used as the reference topographic dataset. We drew thirteen cross-sections along the control reach to compare the PlanetScope-derived DSM with the drone-derived DSM and to support the hydraulic sensitivity analysis (Figure 6b). We then used the two DSMs independently as topographic inputs in 2D hydraulic simulations of the control reach. Six discharges, ranging from 500 to 1300 m³/s, were simulated to evaluate the effect of the topographic input on the resulting water depths.

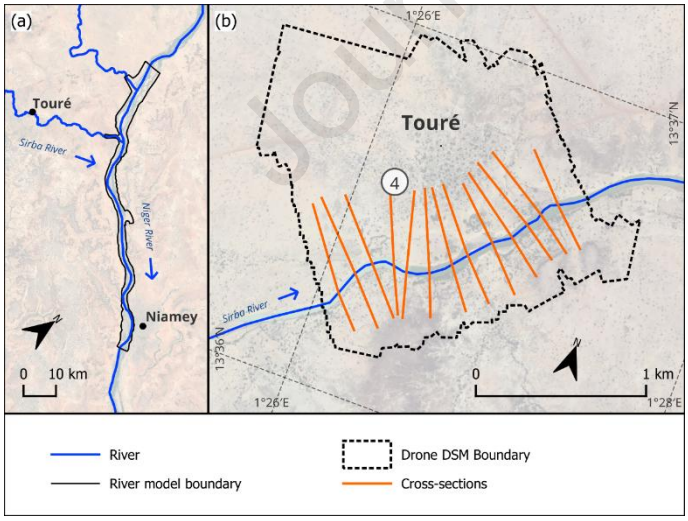

Fig. 6. Sensitivity-analysis site. (a) Touré control reach along the Sirba River relative to the Niger River study area. (b) Drone-derived DSM extent and cross-sections used for the WSE sensitivity analysis; cross-section 4 is shown in Fig. 7.

The mean residual error between simulations based on the PlanetScope and drone DSMs decreased from 0.35 m at Q=500 m³/s to 0.14 m at Q=1300 m³/s, corresponding to approximately 5% of the simulated water depths at the reference high-flow condition. The terrain profiles and the simulated water surface elevation (WSE) for discharges of 750 m³/s and

1200 m³/s were defined as the elevation of the free water surface above sea level, obtained using PlanetScope- and drone-derived DSMs (Fig. 7). Local peaks visible in the WSE profiles are numerical artefacts associated with abrupt elevation discontinuities in the DSM, particularly in the drone-derived surface where small terrain or surface features are represented in greater detail. These local oscillations should therefore not be interpreted as physically meaningful water-level variations; the comparison focuses on the overall agreement between the simulated water levels obtained from the two topographic inputs.

For comparison, an independent roughness-sensitivity test showed that increasing Manning's n from 0.030 to 0.045 produced water-depth changes of the same order, approximately 0.34–0.48 m. The uncertainty associated with the PlanetScope-derived DSM is therefore comparable to the roughness uncertainty expected in 2D hydraulic modelling and does not introduce a disproportionate error into the flood-depth estimates used for the risk analysis.

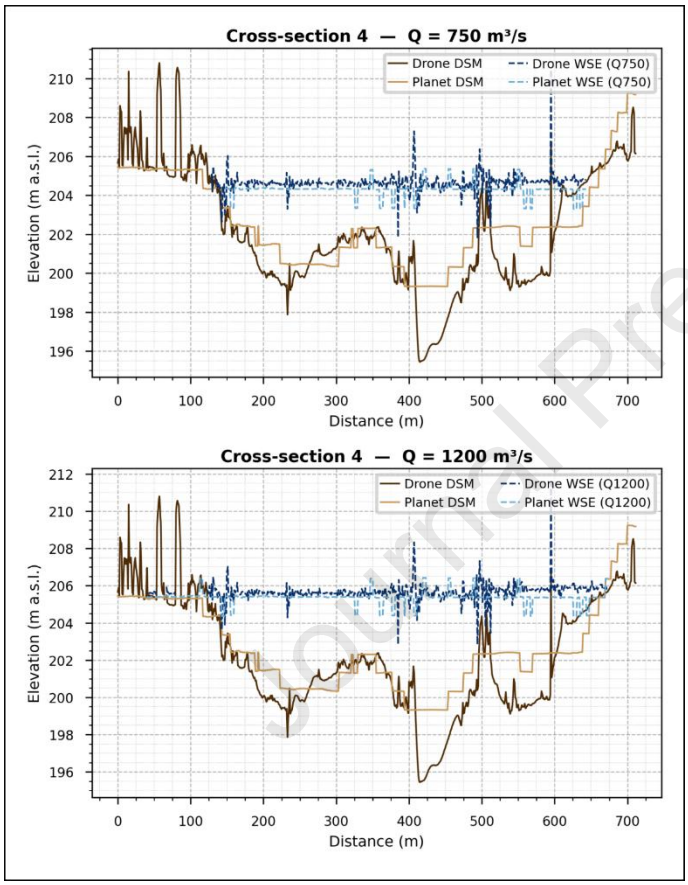

Fig. 7. Terrain profile and simulated water surface elevation (WSE) at cross-section 8 using the Planet-derived DSM and the drone-derived DSM for Q=750 m³/s and Q=1200 m³/s.

2.4.5. Validation

The hazard map was validated by comparing flood inundation edges on 20 August 2024 and 16 February 2025, extracted from Sentinel-2 imagery using the modified normalised difference water index, with the flood area derived from the hydraulic model. These dates correspond to the most recent local and Guinean flood peaks. For each flood, model performance was quantified using the following index [53]:

$F = (Smod \cap Sobs)/(Smod \cup Sobs) \times 100$ (5)

where *Smod* is the predicted inundated area, and *Sobs* is the observed satellite-derived inundated area. *F* values range from 0% to 100%, indicating the degree of spatial agreement between

predicted and observed inundation. Depending on the flood season, the index ranged from 55% to 68% in this study.

2.4.6. Expected damage

ED is defined as the monetary value of physical assets located within the affected area [54]. We identified crops and buildings through visual photointerpretation of Google Earth (GE) imagery. Based on field morphology and cultivation pattern, crops were subsequently classified. Ground verification was conducted in February 2024, when agricultural extension officers randomly sampled and inspected 24 fields. Crops and buildings were identified using the same source (GE) in January 2014 to assess their stability over time.

The damage function of rice crops was defined as the number of submersion days per crop growth stage, with the impact varying by phenological phase. We calculated the ED to agriculture using the average yield of each crop and the corresponding prices, as reported in the Information System on Rural Markets [43]. For buildings, the analysis considered footprint, water depth and flood duration. Notably, the study area's built environment is characterised by single-storey adobe houses, with few structures made of durable materials. These adobe houses lack door thresholds. Consequently, prolonged inundation from Guinean floods led to the partial or total collapse of affected buildings. The ED to buildings was estimated using compensation values stipulated in recent public projects in Niger [43]. Data on georeferenced wells and boreholes were obtained from the statistical service of the Ministry of Environment, Hydraulics and Sanitation.

2.4.7 Risk level

For each local jurisdiction, the risk level was calculated as the product of flood probability and the value of exposed (i) buildings, (ii) wells, (iii) traditional rice, (iv) horticulture in mid-February 2025, and (v) cereals and (vi) pulses in mid-August 2024.

2.5. Risk evaluation

The 15 most common flood risk reduction measures [55–56] were evaluated through a Strengths, Weaknesses, Opportunities and Threats (SWOT) analysis and prioritised on 12 September 2025 in consultation with the mayor, AHA manager, and agricultural extension, water, and sanitation officers from the Gothèye, Karma, Kourteye, and Namaro jurisdictions. We then estimated the number of measures required to reduce flood risk, along with the corresponding costs. These figures were then used to determine the residual risk. The benefit-to-cost ratio included annual per capita savings in healthcare expenses, as reported in the literature [57–59]. We adopted a 10-year horizon, reflecting the typical lifespan of the measures without maintenance, reduced to 4 years for half-moon structures [60]. Each measure was considered implementable within one year. The net present value was therefore calculated using the 5.5% legal discount rate established by the Central Bank of West African States for Niger [61]. When the value exceeds one, risk reduction is considered economically justified.

3. Results

3.1. Risk identification

Notably, recent local floods in the study area have exhibited higher discharge rates and water stages than Guinean-origin floods (Fig. 8). Of the 17 wadis that flow into the Niger River in the section under consideration, the Karma Wadi is the largest and the one that threatens the greatest extent of riverside crops.

Journal Pre-proof

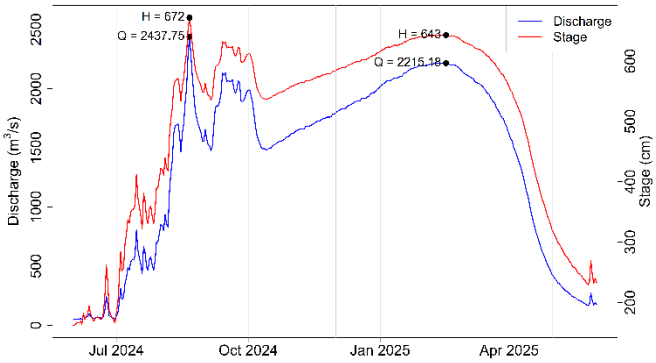

Fig. 8. Hydrograph of the Niger River obtained from the Niamey gauge station during 2024 and 2025.

3.2. Risk analysis

3.2.1 Hazard

River discharge at Niamey during local floods with RPs of 10, 30 and 100 years reached 2,394, 2,637, and 2,858 m^3/s, while Guinean floods reached 2,179, 2,342, and 2,486 m^3/s, respectively (Table S2). Numerical hydraulic modelling indicated that the floodplain in the study area ranged from 119 to 128 km^2. The two flood types exhibited markedly different behaviours. Based on the reconstructed average hydrographs, local floods persisted for approximately 2 days at 99% peak flow and 27 days at 95% peak flow. Conversely, Guinean floods lasted around one month at 99% peak flow and 53 days at 95% peak flow. The estimated Karma Wadi discharge with RPs 10, 30 and 100 (daily precipitation corresponding to 109 mm, 130 mm, and 178 mm) for stream 1 is 629, 930 and 1070 m^3/s and for stream 2 is 27, 39 and 45 m^3/s. The 2012 daily rainfall of 120 mm (~RP20) caused the wadi to flood the Koutoukalé AHA.

3.2.2 Expected damage

A centennial flood occurring between the Dargol–Niger confluence and Niamey could inundate between 809 and 975 ha of irrigated crops, depending on the type of flood and between 28,325 and 49,375 m^2 of buildings. Kourteye is by far the most exposed municipality (Table 3).

Table 3
Exposed assets to local and Guinean floods with an RP of 100 years by municipality.

Municipality	Local		Guinean	
	Buildings footprint m^2	Crops ha	Buildings footprint m^2	Crops ha
Bitinkodji	516	0	0	0
Gothèye	3686	85	6358	109
Karma	1401	147	1315	130
Kourteye	19,893	474	38,845	636
Namaro	2507	104	2857	101
Sum	28,325	809	49,375	975

Traditional rice and horticulture account for 59% and 39% of the exposed area, respectively. Sweet potatoes, pumpkins, corn, and okra collectively account for the remaining 2%. Traditional rice remains the most exposed crop, followed by horticulture (Table S5). During a Guinean flood with an RP of 100 years, 40% of crops and 30% of horticultural areas could be submerged by more than 2 m of water (Table S7). The same event could affect 42 settlements, placing a combined population of 40,000 at risk (Fig. 9, Table S6). The Guinean flood scenario threatens twice the building footprint relative to the local flood.

Journal Pre-proof

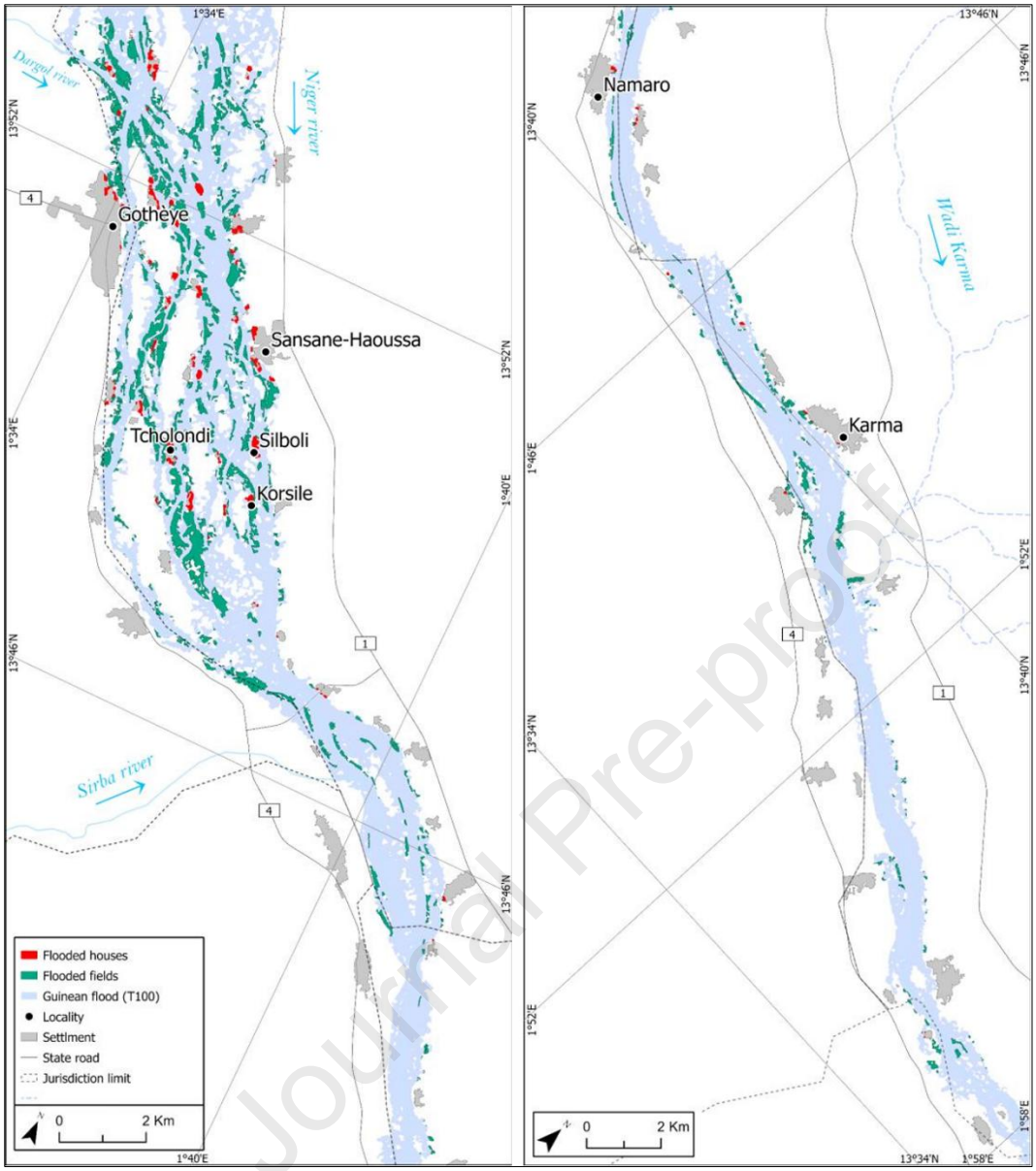

Fig. 9. Exposure map of Guinean floods with RP100 in the Gothèye (left) and Karma (right) sectors.

When both agricultural fields and buildings are considered, Guinean floods cause 30% more ED than local floods. Kourteye is the most affected municipality, accounting for 51%–64% of the total ED, followed by Karma (16%–28%). It also records the highest share of building-related ED, ranging from 38% to 48%, depending on the scenario. Between 57% and 61% of the flood-prone building footprint is concentrated in 10 locations. Korsile, Gothèye, Tcholondi, and Sansane Haoussa are the most at risk under the Guinean RP100 flood. Gothèye, Silboli, Korsile, and Kobadje are the most at risk under the local RP100 flood (Table S6, Fig. 10).
In the event of a once-in-a-century flood, 97 per cent of the building footprint is exposed to a flood depth of less than one metre, with little difference between local and Guinean floods and between municipalities (91–97 per cent), and only 3 per cent would be submerged in water deeper than 2 metres (Table 4).

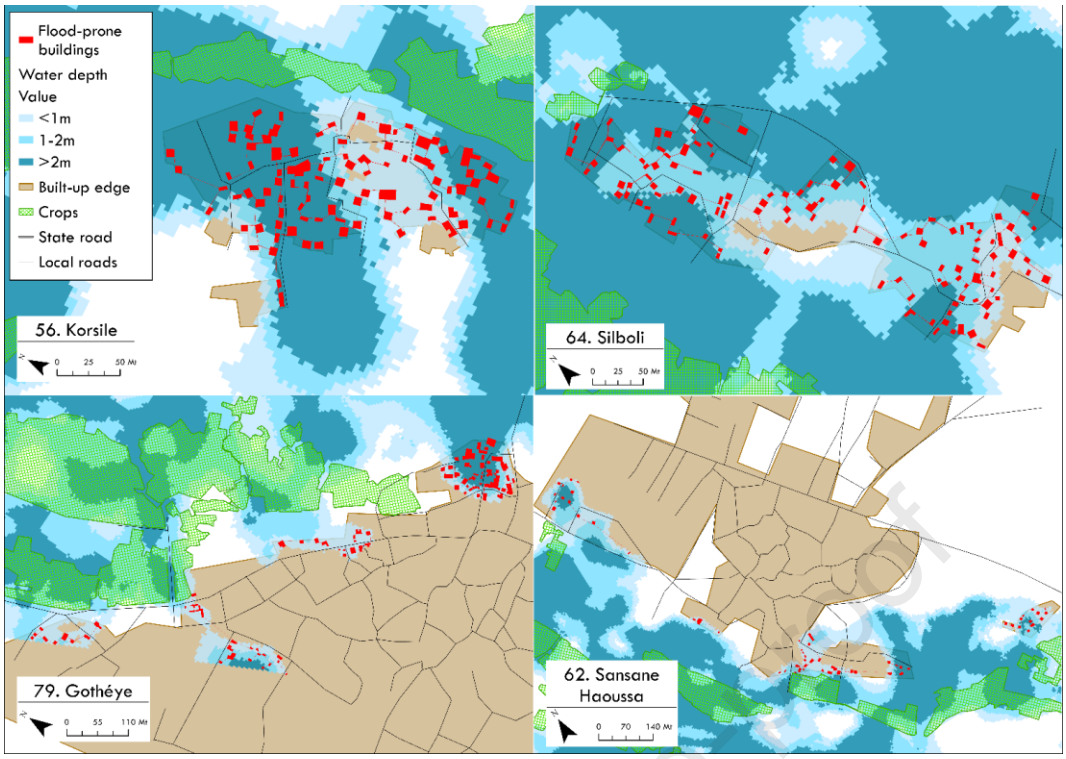

Fig. 10. Buildings susceptible to Guinean RP100 floods in Korsile, Namaro, Sansane Haoussa, and Silboli.

Table 4

Building footprint by inundation depth and municipality in case of local and Guinean floods with RP100 years.

Municipality	Local flood			Guinean flood		
	< 1 m	1–2 m	> 2 m	< 1 m	1–2 m	> 2 m
	%	%	%	%	%	%
Bitinkodji	0	100	0	0	100	0
Gothèye	95	3	2	96	2	2
Karma	94	4	2	92	6	2
Kourteye	97	0	3	97	0	3
Namaro	94	4	2	91	7	1
Sum	97	0	3	97	0	3

The flooding of Karma Wadi with RP10 and RP30 years would inundate 140–146 ha of the 197 ha of the Koutoukalé AHA (Fig. 11). The duration of submersion and the sediments carried by the water result in the complete loss of flooded crops.

Journal Pre-proof

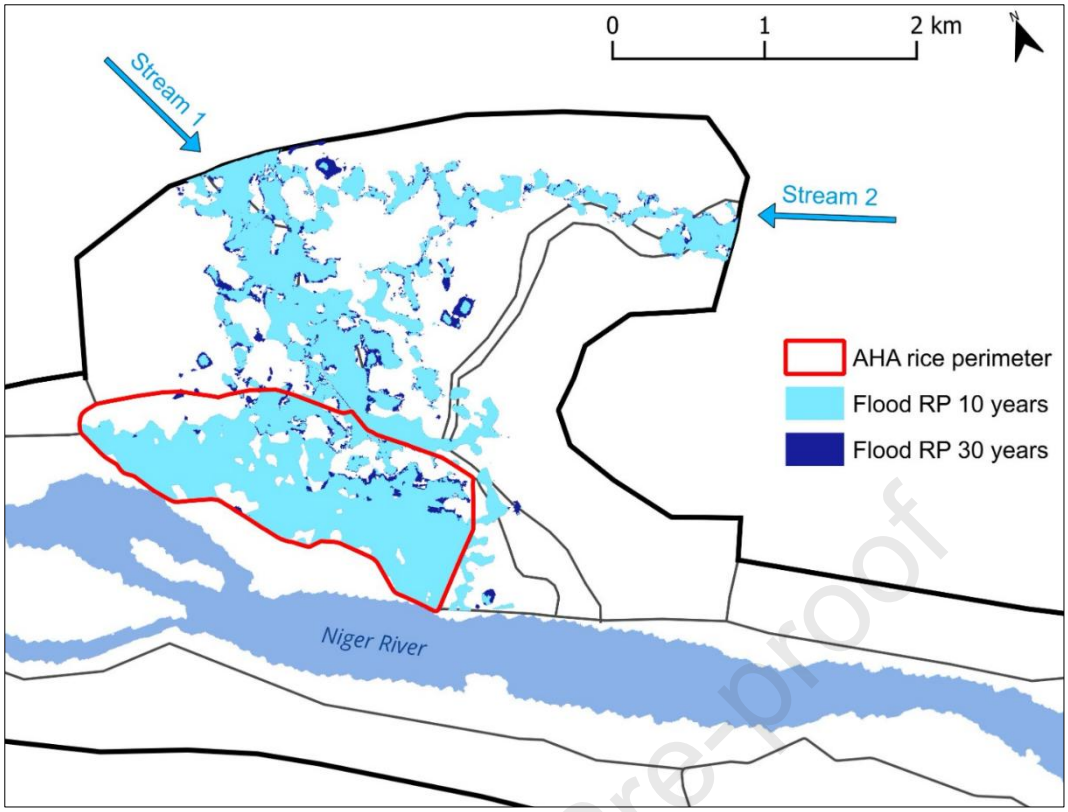

Fig. 11. The Koutoukalé AHA exposure to Karma Wadi flash flood with RP10 and RP30.

The fields remain stable over time, but the settlements do not. If we consider the 13 settlements that account for 71 per cent of the building footprint in the study area, we find that between 2014 and 2024 the number of buildings exposed to a once-in-a-century Guinean flood will increase by 77 per cent and their footprint will increase by 47 per cent. This expansion is more pronounced on the islands than on the coastal localities (Table 5).

Table 5
The 2014–2024 settlements expansion in the inundated area of a Guinean flood RP100.

Human settlement	Buildings exposed to a Guinean flood with an RP of 100 years					
	2014		2024		2014–2024 variation %	
	Number	m^2	Number	m^2	Number	m^2
Silboli	89	3714	115	3974	29	7
Gothèye	57	3111	97	4746	70	53
Korsile	64	2431	95	3527	48	45
Kobadje	48	2399	68	2202	42	-8
Melle Goungou	52	2201	91	2545	52	75
Sokolé	41	1895	73	2543	78	34
Damale	41	1683	61	2301	49	37
Sansane Haoussa	34	1681	76	3395	124	102
Tcholondi	20	1471	54	2336	170	59
Hondobon Goungou	25	1286	43	1788	72	39
Koulbagou	28	1245	49	1664	75	34
Kassani	11	427	78	2208	609	417
Namaro	4	128	12	1588	200	1141
Sum	514	23,672	912	34,817	77	47

3.2.3 Risk level

The Guinean RP10 flood results in the highest risk (€485,000). Kourteye records the highest risk from Guinean flooding (€312,000), followed by Gothèye (€73,000). Karma ranks first for local flooding (€119,000) (Table S12, Fig. 12).

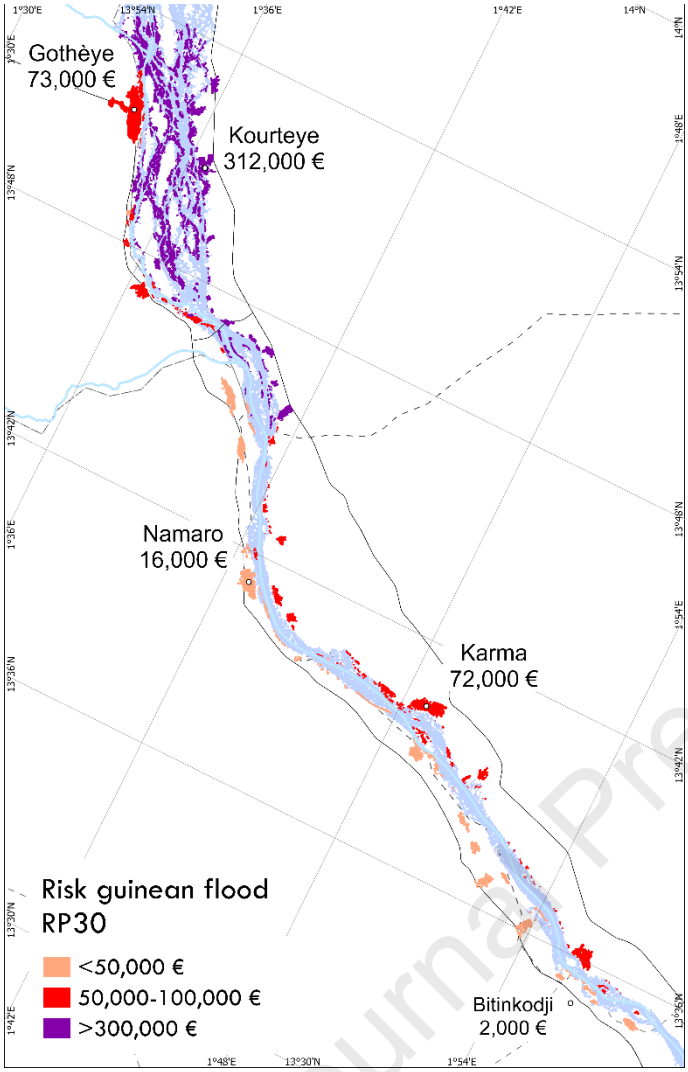

Fig. 12. Risk associated with the Guinean RP10 flood.

3.3. Risk evaluation

The SWOT analysis of 15 standard measures to reduce flood risk (Table S13) and the prioritisation of measures carried out with local authorities (Table S14) considered hazard and exposure maps, municipal emergency plans and an early flood warning system to be useful, although maps were not applicable at the level of individual communities. Implementation opportunities may arise through development aid (Table S13). The open-access dataset on which this FRA is based is described in detail [62], as it is aimed at researchers and practitioners. Structural measures depend on inundation depth. This suggests that horticulture sites could be relocated to higher ground to protect them from Guinean floods lasting one month and causing inundation exceeding 1 m in depth, provided suitable soil and irrigation are available. Buildings susceptible to inundation by water levels below 0.5 m during local floods (Table S9) can be protected with mobile entrance barriers and sandbags around adobe walls. Latrines, wells, and boreholes should be elevated. However, these measures are inadequate for Guinean floods of similar depth due to their extended duration. In such cases, and for floods that produce inundation depths between 1 and 2 m, levees are recommended. Residents of buildings exposed to water depths above 2 m should be relocated. A non-floodable zone should be identified for each settlement expansion. On islands, safe land for settlement expansion is often scarce or

absent, except within already developed areas (Fig. 10). The Koutoukalé AHA should be protected from Karma Wadi floods by managing runoff from the highlands, which cover 35% of the basin's surface (Table S15). Typically, areas with slopes below 5% are treated using trapezoidal bunds and half-moons, but only 692 ha have been treated, 57% of which are in low-lying zones. Gabions are recommended to protect the wadi banks alongside the AHA from erosion [56,63] (Fig. 13 and 14).

Fig. 13. Wadi Karma on 9 November 2025. Photograph by Abdoul Samadou Souley Issa.

Fig. 14. Entry point of the flash flood into the Koutoukalé AHA at the bank of Wadi Karma. Photograph by Abdoul Samadou Souley Issa.

These measures should be extended to the highlands nearest the AHA, totalling 5,204 ha, using trapezoidal bunds and half-moons for pastoral and forestry use (Fig. 15).

Journal Pre-proof

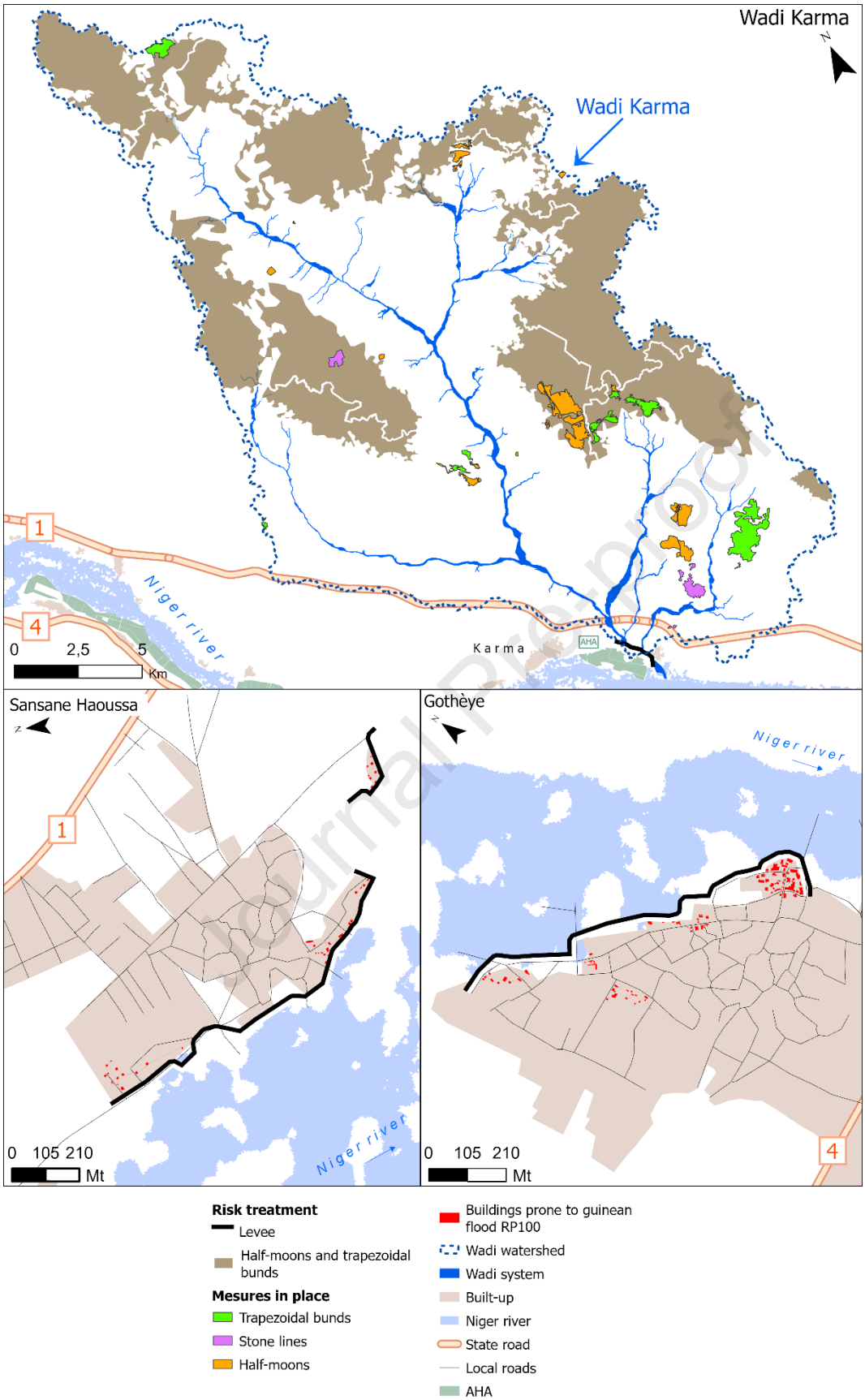

Fig. 15. Risk reduction measures for Karma Wadi, Sansane Haoussa and Gothèye.

Journal Pre-proof

Sandbags, restoration and extension of AHA levees, gabions, half-moons, and trapezoidal bunds in the Karma Wadi catchment, sanitation, hygiene, early warning system, flood warning signage, and stages are priorities, whereas resettlement, relocating crops to higher ground, polders, and entrance flood barriers rank lowest (Table S14).

The treatment for local RP10 floods involves raising and reinforcing the existing levees along the AHA and extending them to protect against overflow from the Sirba River and Karma Wadi. The treatment of Guinean floods includes protecting buildings exposed to water depths of up to 1 m using sandbags and levees, and replacing latrines with elevated, improved models. These measures are intended to cover half of the exposed building footprint. Beyond protecting buildings, these interventions aim to safeguard public health during floods, which often lead to diarrhoea, typhoid fever, and death [64]. In Kourteye, the risk of Guinean RP10 flood is projected to decrease from level 100 to 69 following treatment. Similarly, the Guinean RP100 flood risk can be reduced to 63 in Namaro. The same local jurisdictions do not fall below 75 for local RP10 and RP100 floods. (Tables 6, S16).

Table 6
Residual risk from Guinean RP10 and RP100 floods.

Flood type and frequency	Risk (R) Residual risk (RR)	Bitinkodji K €	Gothèye K €	Karma K €	Kourteye K €	Namaro K €	Total K €
Local RP10	R	5	47	119	230	17	417
	RR	5	42	119	191	12	371
	RR index (R=100)	100	91	100	83	75	89
Local RP100	R	1	7	13	21	4	42
	RR	1	6	10	16	3	16
	RR index (R=100)	100	89	76	75	76	86
RP10	R	2	74	72	320	17	485
	RR	2	55	72	221	12	381
	RR index (R=100)	100	74	100	69	75	78
RP100	R	1	9	9	29	5	58
	RR	1	8	9	24	3	44
	RR index (R=100)	100	87	100	82	63	80

In AHAs, raising and reinforcing levees with stone cladding, extending them, protecting 600 m of the Wadi Karma left bank with gabions, and treating the highlands of the Karma basin using half-moons and trapezoidal bunds incur costs (Table S17). Meanwhile, benefits include avoided harvest losses during flooding and fodder yield from the treated highlands. In settlements, costs include building protection with sandbags and levees, signage in flood-prone areas, stages to monitor river levels, and replacing latrines with elevated, improved models. The corresponding benefits include safeguarding buildings exposed to water depths of up to 1 m and annual healthcare savings of up to €10 per capita [57–59]. Risk reduction is economically justified in Karma and Namaro, but not in Gothèye and Kourteye (Tables 7, S17).

Table 7
Benefit/cost ratio of risk treatment for local and Guinean RP10 and RP100 floods.

Flood type	Location	Gothèye	Karma	Kourteye	Namaro
Local RP10	AHA	-	0.1	-	0.5
	Settlements	0.4	0	0.4	21.2
Local RP100	AHA	-	0.1	-	0.5
	Settlements	0.4	32	0.6	19
Guinean RP10	AHA	-	-	-	-
	Settlements	0.4	1,4	0.6	26
Guinean RP100	AHA	-	-	-	-
	Settlements	0.4	39.9	0.6	26

4. Discussion

Recent studies on FRAs in rural areas of LMICs increasingly rely on outdated, low-resolution geospatial data and lack field validation. Participatory methods and the integration of technical and local knowledge are seldom implemented, diverging from the core principles of the SFDRR. Consequently, measures to reduce river flood risk are rarely identified. The research question focused on how an enhanced FRA could contribute to risk management. The FRA developed herein was improved as follows.

4.1. Holistic, participatory flood risk identification

Participatory threat identification is the first step in a robust FRA and directly informs risk-reduction measures. We considered both river and wadi floods. Multi-hazard assessments in riverine areas remain uncommon, as most studies focus on either river flooding or flash floods. The Guinean flood was found to pose a greater risk than the local flood, despite its lower discharge. This is because most assets are situated upstream of the Sirba–Niger confluence, below which local flood levels rise considerably. Moreover, the Guinean flood submerges extensive horticultural zones that are not irrigated during local floods. This flood persists for a month, while local floods last just two days at 99% of the peak. Finally, AHAs were inundated during local river floods at locations where levees were old or lacked stone cladding. Recently, heavy rainfall triggered flooding of the Karma Wadi at the Koutoukalé AHA, where levees were missing. Most of this knowledge springs from conversations with local stakeholders, field visits, and focus groups with local governments [42]. This confirms that participation and knowledge integration boost risk reduction efforts [65–66], particularly in flood risk management [67].

4.2. High-resolution geoinformation

The PlanetScope-derived DSM improved the accuracy of the modelled flood zone compared to SRTM DEM. The SRTM DEM overestimates flood-prone locations by 36%, ED by 9%–11% for Guinean floods and between 13%–18% for local floods (Table S10). The discrepancy between PlanetScope-derived and SRTM DEMs arises because the multiple narrow channels of the Niger River upstream of the Sirba confluence cannot be resolved by DEMs with a resolution of 30 m. High-resolution (~0.5 m) freely available imagery, combined with field inspections, enabled the identification of buildings and crops. Such detail is seldom achieved in comparable assessments. This level of detail makes it possible to observe over the last 10 years the distance of crops and buildings from flooding. The fields have remained relatively stable over time, whilst in the thirteen most exposed settlements, the number of buildings in the centennial flood-prone zone and their total floor area have increased by 77 per cent and 47 per cent respectively, confirming a trend observed in several countries [68]. This trend is significantly more pronounced on the islands. These sites are highly sought-after because they are close to water all year round, making them particularly suitable for agriculture in a semi-arid context. By contrast, the islands have few sites above the 100-year flood level.

The high resolution of the DSM helps to refine flood depth estimates compared with the SRTM and ALOS PALSAR DEMs currently used in LMICs. Uncertainty in flood depth strongly affects damage estimates [69]. Flood depth and duration are also closely linked to identifying risk-reduction measures. In the study area, 97 per cent of assets are exposed to less than one metre of water for at least one month. This condition is rarely considered in FRAs in LMICs. Consequently, the literature quantifying the potential impact of flooding in LMICs according to flood depth is still limited [70].

4.3. Local scale

Conducting risk assessment at the local-jurisdiction scale improved its relevance to decision-making. However, such detail remains uncommon [71–73] in contrast to studies that delineate local jurisdictions without specifying the level of risk for each [74–82].

4.4. Participatory identification of measures

The literature on FRAs in rural regions of LMICs rarely addresses participatory selection of measures. Raising of AHA levees was a priority, as confirmed in the literature [73,79,82–84]. An EWS was equally essential [29,77,79,82,84–85]. Sanitation and hygiene were ranked second but rarely recommended in the literature on river flood risk [29,77,86]. Flood signals, suggested in the literature [29,75], were reported to be vulnerable to damage or theft. Flood depth-damage maps were often difficult for local communities to interpret, contrary to reports in the literature. This is because maps simply overlay assets on water depth without familiar reference points for residents. These measures were estimated to substantially reduce Guinean RP10 flood risk in Kourteye and RP100 flood risk in Namaro. In the other municipalities, residual risk remained at around 75% of the pre-treatment level. Greater reduction would require resettlement and relocating crops to higher ground. However, restricting development in flood-prone areas, resettlement [80], and redirecting land development [81,84,87], which have socio-economic disadvantages [88], were not applicable along the River Niger because residents are attached to their land and relocation is costly. Annually, the cost of risk treatment was lower than the benefit in Karma and Namaro, whereas in AHAs it equals or exceeds the benefit.

Limited availability of land for resettlement and crop relocation was an unexpected finding. This creates challenges for local governments in securing land to relocate exposed communities and agricultural activities.

Although this FRA used high-resolution geoinformation and participatory processes, it has certain limitations. We had to use discharge data from Garbey Kourou station as a proxy for Kakassi station. This was justified using consolidated methods; however, it inevitably increases uncertainty in the results. Moreover, hourly rainfall data for the Karma catchment were derived by theoretically scaling down the daily data, introducing additional uncertainty. The few buildings constructed with durable materials could not be isolated, and the impact of stormwater on adobe houses could not be quantified. Finally, it was impossible to quantify the need for flood-proof, heavy-rain-resistant community shelters (generally, schools built with durable materials). Consequently, the flood risk was underestimated.

Overall, the FRA findings have five key implications. 1) Protecting AHA and agriculture from flooding is not cost-effective, but it prevents food insecurity and rural poverty. 2) Participatory, high-resolution FRAs facilitate the transition to an impact-based EWS. 3) The inundation depth-damage data supports flood prevention, preparation, response, rescue, and recovery operations. 4) Inundation depth-damage maps can be directly applied to risk zoning in local and regional emergency plans. 5) The stability of crops over time means that updating field data is less urgent, but the rapid growth of settlements suggests that the built environment should be monitored more frequently.

The recommendations primarily focus on land access, a topic overlooked in the literature but central to risk reduction. Second, risk reduction should be implemented within an FRA framework. Finally, we recommend reactivating the Kakassi hydrological station and installing a new hydrological station in Farié to begin measuring river discharge well before the floods reach Niamey.

Journal Pre-proof

5. Conclusion

This study aimed to address persistent shortcomings in flood hazard identification, participatory processes and risk reduction strategies within FRAs conducted in rural regions of LMICs over the past decade. We examined how an enhanced FRA could improve flood risk management by using a participatory approach that integrates high-resolution geoinformation and local knowledge when field inspection opportunities are limited.

Our assessment covered a rural area extending 58 km along the Niger River, upstream of Niamey, and a 381 km² catchment encompassing the largest wadi tributary. The flood hazard was multifaceted. Flood-prone settlements and assets were far fewer in number when estimated using the PlanetScope-derived DSM than when identified using the SRTM DEM. Between 2014 and 2024, the number of buildings exposed to a once-in-a-century Guinean flood will increase by 77%, and their footprint by 47%. We assessed risk by identifying assets exposed to flood depths and evaluating their value. This enabled us to identify and prioritise appropriate risk-reduction measures. Extending the levee system, together with implementing a performant EWS, emerged as the top priority. Sanitation and hygiene measures followed, although they are not typically recommended in FRAs. Resettlement, although frequently proposed in the literature as a strategy to reduce flood risk in rural areas of LMICs, was found to be unfeasible. Our findings highlight future research directions on land access and updating the FRA. Our study has practical implications for preventing food insecurity and rural poverty, delivering impact-based EWSs, and supporting local and regional emergency planning, as well as flood preparedness, response, and recovery operations.

Detailed mesoscale flood risk assessments, including hotspot identification and suitable risk reduction strategies, are achievable when the process is participatory, technically robust, and informed by local knowledge.

CRediT authorship contribution statement

M. Tiepolo: Conceptualisation, data curation, funding acquisition, investigation, methodology, supervision, writing-original draft, writing-review & editing. **M. Abraiz:** Formal analysis, investigation, writing-original draft. **M.H. Housseini:** Data curation, investigation. **O. Baoua**: Investigation. **E. Belcore:** Methodology. **G. Cannella:** Data curation, investigation, validation, visualisation. **D. Ganora:** Conceptualisation, methodology, formal analysis. **A. Marmolejo Gutiérrez:** Formal analysis, investigation, writing-original draft, writing review. **M. Piras:** Conceptualisation, methodology, resources. **F. Saretto:** Formal analysis, investigation, writing-original draft. **R. Vesipa:** Conceptualisation, methodology, software, resources, writing review.

Funding
This work was supported by the SLAPIS project funded by the Italian Development Cooperation Agency (AID 12487)

Appendix A. Supplementary material
Supplementary data to this article can be found online at https://data.mendeley.com/datasets/9v349h653n/6

References
[1] J. Leaning, D. Guha-Sapir, Natural disasters, armed conflict, and public health, New Eng. J. Med. 369 (2013) 1836–1842. https://doi.org10.1056/NEJMra1109877.
[2] United Nations, Sendai framework for disaster risk reduction 2015-2030, UNDRR, Geneva (Switzerland), 2015.
[3] J. Martinez-Alier, I. Anguelovski, P. Bond, D. Del Bene, F. Demaria, J.-F. Gerber, L. Greyl, W. Haas, H. Healy, V. Marin-Burgos, G. Ojo, M. Porto, L. Rijnhouit, B. Rodriguez-Labajos, J. Spangenberg, L. Temper,

R. Warlenius, I. Yánez, Between activism and science: grassroots concepts for sustainability coined by environmental justice organizations, J. Pol. Ecol. 21 (2014) 19–60. https://doi.org/102458/v21i1.21124.

[4] D. Roberts, Thinking globally, acting locally – institutionalizing climate change at the local government level in Durban, South Africa, Environ. Urbanization 20 (2008) 521–537. https://doi.org/10.1177/0956247808096126.

[5] S.V.R.K. Prabhakar, A. Srinivasan, R. Shaw, Climate change and local level disaster risk reduction planning: need, opportunities and challenges, Mitig. Adapt. Strateg. Glob. Change 14 (2009) 7–33. https://10.1007/s11027-008-9147-4.

[6] J. Coburn, Environmental justice, local knowledge, and risk: the discourse of a community-based cumulative exposure assessment, Environ. Manag. 29 (2002) 451–466. https://doi.org/10.1007/s00267-001-0013-3.

[7] M. Pelling, Learning from others: the scope and challenges for participatory disaster risk assessment, Disasters 31 (2007) 373–385. https://doi.org/10.1111/j.0361-3666.2007.01014.x.

[8] M.K. Van Aalst, T. Cannon, I. Burton, Community level adaptation to climate change: The potential role of participatory community risk assessment, Glob. Environ. Chang. 18 (2008) 165–179. https://doi.org/10.1016/j.gloenvcha.2007.06.002.

[9] J.C. Gaillard, J. Mercer, From knowledge to action: Bridging gaps in disaster risk reduction, Progress Human Geo. 37, (2013) 93–114. https://doi.org/10.1177/0309132512446717.

[10] L. Hiwasaki, E. Luna, Syamsidik, R. Shaw, Process for integrating local and indigenous knowledge with science for hydro-meteorological disaster risk reduction and climate change adaptation in coastal and small island communities, Int. J. Disaster Risk Reduct. 10 (2014) 15–27. http://dx.doi.org/10.1016/j.ijdrr.2014.07.007.

[11] M.B. Kia, S. Pirasteh, B. Pradhan, A.R. Mahmud, W.N.A. Sulaiman, A. Moradi, An artificial neural network model for flood simulation using GIS: Johor River Basin, Malaysia, Environ. Earth Sci. 67 (2011) 251–264. https://doi.org/10.1007/s12665-011-1504-z.

[12] M.S. Teherany, B. Pradhan, S. Mansor, N. Ahmad, Flood susceptibility assessment using GIS-based support vector machine model with different kernel types, Catena 215 (2015) 91–101. https://doi.org/10.1016/j.catena.2014.10.017.

[13] J.H. Danumah, S.N. Odai, B.M. Saley, J. Szarzynski, M.M. Thiel, A. Kwaku, F.K. Kouame, L.Y. Akpa, Flood risk assessment and mapping in Abidjan district using multi-criteria analysis (AHP) model and geoinformation techniques, (cote d'ivoire), Geoenviron. Disasters 3 (2016) 10. https://doi.org/10.1186/s40677-016-0044-y.

[14] S. Chakaborty, S. Mukhopadhyay, Assessing flood risk using analytical hierarchy process (AHP) and geographical information system (GIS): application in Coochbehar district of West Bengal, India, Nat. Haz. 99 (2019) 247–274. https://doi.org/10.1007/s11069-019-03737-7.

[15] R.W. Saaty, The analytical hierarchy process–what it is and how it is used, Math. Modelling 3–5 (1987) 161–176.

[16] B. Büchele, K. Kreibich, A. Kron, A. Thieken, J. Ihringer, O. Oberle, B. Merz, F. Nestmann, Flood-risk mapping: contributions towards an enhanced assessment of extreme events and associated risks, Nat. Haz. Earth Syst. Sci. 6 (2006) 485–503. www.nat-hazards-earth-syst-sci.net/6/485/2006/

[17] H. Apel, T. Aronica, H. Kreibich, A.H. Thieken, Flood risk analyses—how detailed do we need to be? Nat. Haz. 49 (2009) 79-98. https://doi.org/10.1007/s11069-008-9277-8.

[18] M. Masood, K. Takeuchi, Assessment of flood hazard, vulnerability and risk of mid-eastern Dhaka using DEM and 1D hydrodynamic model, Nat. Haz. 61 (2012) 757–770 https://doi.org/10.1007/s11069-011-0060-x.

[19] Y.S. Getahun, S.L. Gebre, Flood Hazard Assessment and Mapping of Flood Inundation Area of the Awash River Basin in Ethiopia using GIS and HEC-GeoRAS/HEC-RAS Model, J. Civil Environ. Eng. 5 (2015) 4. https://doi.org/10.4172/2165-784X.1000179.

[20] P.A. Brivio, R. Colombo, M. Maggi, R. Tomasoni, Integration of remote sensing data and GIS for accurate mapping of flooded areas, Int. J. Rem. Sens., 23 (2000) 429–441. https://doi.org/10.1080/01431160010014729.

[21] C.L. Vishnu, K.S. Sajinkumar, T. Oommen, R.A. Coffman, K.P. Thrivikramji, V.R. Rani, S. Keerthy (2019) Satellite-based assessment of the August 2018 flood in parts of Kerala, India, Geomatics, Nat. Haz. Risk, 10 (2019) 758–767. https://doi.org/10.1080/19475705.2018.1543212 2019.

[22] K. Jacobsen, Digital elevation models – From satellite images to free available DEMs, Int. Arch. Photogram. Rem. Sens. Spatial Info. Sci. XLVIII-M-6–2025 (2025) 147–152. https://doi.org/10.5194/ISPRS-ARCHIVES-XLVIII-M-6-2025-147-2025.

[23] F. McClean, R. Dawson, C. Kilsby, Implications of using global digital elevation models for flood risk analysis in cities, Water Resour. Res. 56 (2020) e2020WR028241. https://doi.org/10.1029/2020WR028241;SUBPAGE:STRING:FULL.

[24] M.M. Bennett, C.J. Gleason, K.K. Friedrich, B. Tellman, U. Ovienmhada, L.F. Alvarez Leon, A.J. Mathews, Bringing satellites down to Earth: six steps to more ethical remote sensing. Glob. Environ. Chang Advances. 2 (2024) 100003. https://doi.org/10.1016/j.gecadv.2023.100003.

Journal Pre-proof

[25] K. Ali, R.M. Bajracharya, H.L. Koirala, A review of flood risk assessment, Int. J. Environ. Agric. Biotech. 1 (2016) 1065–1077. http://dx.doi.org/10.22161/ijeab/1.4.62.

[26] A. Almoradie, M.M. de Brito, M. Evers, A. Bossa, M. Lumor, C. Norman, Y. Yacouba, J. Hounkpe, 2019. Current flood risk management practices in Ghana: Gaps and opportunities for improving resilience, J. Flood Risk Manag. 13, e12664. https://doi.org/10.1111/jfr3.12664.

[27] N.A. Alias, C. Siwar, M.K. Ismail, N.D.M. Idris, Flood disaster management in Sungai Pahang basin: case of Temerloh, in: Z. Yusop, A. Aris, N.E. Alias, K.V. Annammala, WL. Waugh (Eds.), Improving flood management, prediction and monitoring: case studies in Asia, Emerald publishing, Leeds (England), 2018, pp. 91–102. https://doi.org/10.1108/S2040-726220180000020017.

[28] B. Bwambale, M. Muhumuza, M. Nyeko, Traditional ecological knowledge and flood risk management: A preliminary case study of the Rwenzori. Jàmbá J. Disaster Risk Stu. 10 (2018) a536. https://doi.org/10.4102/jamba.v10i1.536Chambre 2018.

[29] M. Tiepolo, M. Rosso, G. Massazza, E. Belcore, S. Issa, S. Braccio, Flood assessment for risk-informed planning along the Sirba River, Niger, Sustainability 11 (2019) 4003. https://doi.org/10.3390/su11154003.

[30] M. Tiepolo, S. Braccio, E. Fiorillo, A. Galligari, G.L. Katiellou, G. Massazza, V. Tarchiani, Participatory risk assessment of pluvial floods in four towns of Niger, Int. J. Disaster Risk Reduct. 84 (2023) 103454. https://doi.org/10.1016/j.ijdrr.2022.103454.

[31] D. Eilander, A. Couasnon, F.C. Sperna Weiland, W. Ligtvoet, A. Bouwman, C. Hessel, H.C. Winsemius, P.J. Ward, Modeling compound flood risk and risk reduction using a globally applicable framework: a pilot in the Sofala province of Mozambique, Nat. Haz. Earth Sys. Sci. 23 (2023) 2251–2272. https://doi.org/10.5194/nhess-23-2251-2023.

[32] V. Amarakoon, G. Dharmarathne, R. Premasiri, M. Mukherjee, R. Shjaw, D. Wickramasinghe, Potential for the complementary and integrative use of citizen science and modern science in flood risk reduction: a case study from Sri Lanka, Int. J. Disaster Risk Reduct. 103 (2024) 104331. https://doi.org/10.1016/j.ijdrr.2024.104331.

[33] A.E. Putriasri, L. Eliasta, S.I. Amatullah, C. Sandi, A.R. Pahlevi, S.N. Hikmat, I. Jaya, B. Kosasih, A. Rahmawati, Y. Hermawan, Giujung river basin flood risk assessment due to climate change and its countermeasures, IOP conf Ser. Earth Environ. 1343 (2024) 012037. https://doi.org/10.1088/1755-1315/1343/1/012037.

[34] G. Massazza, M. Bacci, L. Descroix, M.I, Housseini, E. Fiorillo, G.L. Katiellou, G. Panthou, A. Pezzoli, M. Rosso, E. Sauzedde, A. Terenziani, T. De Filippis, L. Rocchi, S. Burrone, M. Tiepolo, T. Vischel, V. Tarchiani, Recent changes in hydroclimatic patterns over medium Niger River basins at the origin of the 2020 Flood in Niamey (Niger), Water. 13 (2021) 1659. https://doi.org/10.3390/w13121659.

[35] République du Niger, Institut National de la Statistique, Répertoire national des localités (ReNaLoc), NS, Niamey, 2014. https://www.stat-niger.org/wp-content/uploads/renaloc/ReNaLoc_RGPH_2012.pdf.

[36] International Electrotechnical Commission, International Organization for Standardization, International standard IEC/ISO 31010 Risk management – Risk assessment techniques, International Electrotechnical Commission, Geneva (Switzerland), 2009

[37] S.N. Jonkman, M. Bockarjova, M. Kok, P. Bernardini, Integrated hydrodynamic and economic modelling of flood damage in the Netherlands, Ecol. Econ. 66 (2008) 77–90. https://doi.org/10.1016/j.ecolecon.2007.12.022.

[38] H. De Moel, J. van Alphen, J.C.J.H. Aerts, Flood maps in Europe–methods, availability and use, Nat. Haz. Earth Syst. Sci. 9 (2009) 289–301. https://doi.org/10.5194/nhess-9-289-2009.

[39] B. Merz, H. Kreibich, A. Thieken, R. Schmidtke, Estimation uncertainty of direct monetary flood damage to buildings, Nat. Haz. Earth Syst. Sci. 4 (2004) 153–163. https://doi.org/10.5194/nhess-4-153-2004.

[40] J. Birkmann, T. Welle, Assessing the risk of loss and damage: exposure, vulnerability and risk to climate-related hazards for different country classifications, Int. J. Glob. Warm. 8 (2015) 191–212. https://doi.org/10.1504/IJGW.2015.071963.

[41] M. Tiepolo, S. Braccio, Local and scientific knowledge integration for multi-risk assessment in rural Niger, in: M. Tiepolo, A. Pezzoli, V. Tarchiani (Eds.), Renewing local planning to face climate change in the tropics, Springer, Cham Switzerland, 2017, pp. 227–245.

[42] S. Sigourou, P. Dimitriadis, V. Pagana, A. Tsouni, T. Iliopoulou, G.-F. Sargentis, R. Ioannidis, D. Dimitrakopoulou, E. Chardavellas, N. Mamassis, D. Koutsoyiannis, C.H. Kontoes, Developing an integrated methodology for flood-hazard assessment: application to the Pikrodafni River Basin (Attica, Greece), Front. Built Environ. 12 (2026) 1768439. https://doi.org/10.3389/fbuil.2026.1768439.

[43] M. Tiepolo, M. Abraiz, M. Bacci, O. Baoua, E. Belcore, G. Cannella, E. Fiorillo, D. Ganora, I.M. Housseini, G.L. Katiellou, M. Piras, V. Tarchiani, Flood damage risk mapping along the River Niger: ten benefits of a participated approach, Clim. 13 (2025) 80. https://www.mdpi.com/2225-1154/13/4/80.

[44] J.R.M. Hosking, J.R. Wallis, Regional frequency analysis: An approach based on L-moments, Cambridge University Press, 1997.

Journal Pre-proof

[45] M. Marani, M. Ignaccolo, A metastatistical approach to rainfall extremes, Advances Water Resour. 79 (2015) 121–126. https://doi.org/10.1016/j.advwatres.2015.03.001.
[46] V.T. Nguyen, D. Georges, G. Besançon, Application of variational calculus to parameter estimation in a real hydrological system, Eur. J. Control 60 (2021) 11–19. https://doi.org/10.1016/j.ejcon.2021.03.009.
[47] M.S. Kappes, M. Keller, K. von Elverfeldt, T. Glade, Challenges of analyzing multi-hazard risk: a review, Hat. Haz. 64 (2010) 1925-1958. https://doi.org/10.1007/s11069-012-0294-2.
[48] M. Abraiz, E. Belcore, M. Piras, DEM generation from multi-view satellite images in Sub-Sahel Region, Int. Archives Photogrammetry Rem. Sens. Spatial Info. Sci. (2025) XLVIII-M-6-2025. https://doi.org/10.5194/isprs-archives-XLVIII-M-6-2025-9-2025.
[49] D. Vanzo, S. Peter, L. Vonwiller, M. Bürgler, M. Weberndorfer, A. Siviglia, D. Conde, D.F. Vetsch BASEMENT v3: a modular freeware for river process modelling over multiple computational backends, Environ. Model. Software 143 (2021) 105102. https://doi.org/10.1016/j.envsoft.2021.105102.
[50] G. Choné, P.M. Biron, T. Buffin-Bélanger. Flood hazard mapping techniques with LiDAR in the absence of river bathymetry data, E3S Web Conferences 40 (2018) 06005. https://doi.org/10.1051/e3sconf/20184006005.
[51] V.T. Chow, Open-channel hydraulics, McGraw-Hill, New York (USA), 1959.
[52] E. Belcore, M. Piras, A. Pezzoli, G. Massazza, M. Rosso, Raspberry PI 3 multispectral low-cost sensor for UAV based remote sensing. Case study in South-west Niger, Int. Arch. Photogramm. Remote Sens. Spatial Inf. Sci. XLII-2/W13 (2019) 207–214. https://doi.org/10.5194/isprs-archives-XLII-2-W13-207-2019.
[53] M.S. Horritt, P.D. Bates, Evaluation of 1D and 2D numerical models for predicting river flood inundation, J. Hydrol. 268 (2002) 87–99. https://doi.org/10.1016/S0022-1694(02)0 0121-X.
[54] World Health Organisation, Glossary of health emergency and disaster risk management terminology, WHO, Geneva (Switzerland), 2020.
[55] P. Sayers, L. Yuanyuan, G. Galloway, E. Penning-Rowsell, S. Fuxin, W. Kang, C. Yiwei, T. Le Quesne, Flood risk management. A strategic approach, UNESCO, Paris, 2013.
[56] W. Critchley, K. Siegert, A manual for the design and construction of water harvesting schemes for plant production, FAO, Rome, 1991. https://www.fao.org/4/u3160e/u3160e00.htm.
[57] Water and Sanitation Program, 2012. Le Niger perd 75 milliards XOF chaque année à cause d'un mauvais assainissement. https://documents1.worldbank.org/curated/en/627261468124151217/pdf/684660WSP0ESI00ch00PUBLIC00brochure.pdf (accessed 1 November 2025).
[58] P. Dasgupta, S. Sahay, A. Prakash, A. Lutz, Cost effective adaptation to flood: sanitation interventions in the Gandak river basin, India, Clim. Develop. 12 (2020) 717–729. https://doi.org/10.1080/17565529.2019.1682490.
[59] R. Brouwer, D.F. Sharmin, S. Elliott, J. Liu, M.R. Khan, Costs and benefits of improving water and sanitation in slums and non-slum neighborhoods in Dhaka, a fast-growing mega-city, Ecol. Econ. 207 (2023) 107763. https://doi.org/10.1016/j.ecolecon.2023.107763.
[60] A. Abdou, S.C. Abdoulahi, M.A. Tidjani, M.S. Hassimi, A.K.A. Sabra, A.E. Soulé, M. Kaire, Économie de la dégradation des terres à Tahoua, Niger. Analyse coût-bénéfice des activités de récupération des terres (banquettes, demi-lunes et cordons pierreux) des quatre sites de la commune rurale de Badaguichiri. 2019. https://spn2a.org/wp-content/uploads/2020/05/ELD-NIG_Rapport_Tahoua_2019-11-22-ELD-Niger-report-INRAN-web.pdf.
[61] Banque Centrale des États de l'Afrique de l'Ouest, Taux d'intérêt légal 2025 des pays de l'UMOA, 2025. https://www.bceao.int/fr/documents/taux-dinteret-legal (accessed 1 November 2025).
[62] M. Tiepolo, G. Cannella, M. Abraiz, O. Baoua, E. Belcore, D. Ganora, M.I. Housseini, A. Marmolejo Gutierrez, M. Piras, F. Saretto, R. Vesipa, Dataset on flood risk along the Niger River upstream of Niamey. Data 11 (2026) 132. https://doi.org/10.3390/data11060139.
[63] République du Niger, Ministère de l'environnement et de lutte contre la désertification, Recueil de fiches techniques de bonnes pratiques de gestion durable des terres (GDT) au Niger, 2022. https://niger-gdte.net. (accessed 30 Octobre 2025).
[64] United Nations Office for the Coordination of Humanitarian Affairs, Responding to floods in Niger, 2021. https//www.unocha.org/publication/report/niger/responding-floodss.-niger (accessed 30 October 2025).
[65] T.D.G. Hermans, R.S. Trogrlic, M.J.C. van den Homberg, H. Bailon, A. Mosurska, Exploring the integration of local and scientific knowledge in early warning systems for disaster risk reduction: a review, Nat. Haz. 114 (2022) 1125–1152. https://doi.org/10.1007/s11069-022-05468-8.
[66] K. Vasileiou, J. Barnett, D. Stanton, Integrating local and scientific knowledge in disaster risk reduction: A systematic review of motivations, processes, and outcomes, Int. J. Disaster Risk Reduct. 81 (2022) 103255. https://doi.org/10.1016/j.ijdrr.2022.103255.
[67] S.A. Maskrey, N.J. Mount, C.R. Thorne, Doing flood risk modelling differently: Evaluating the potential for participatory techniques to broaden flood risk management decision-making, J. Flood Risk Manag. 15 (2021) e12757. https://doi.org/10.1111/jfr3.12757.

Journal Pre-proof

[68] N. Wang, F. Sun, D. Koutsoyiannis, T. Iliopopulou, T. Wang, H. Wang, W. Liu, G.-F. Sargentis, P. Dimitriadis, How can changes in the human-flood distance mitigate flood fatalities and displacements? Geophysical Res. Letters, 50 (2023) e2023GL105064. https://doi.org/10.1029/2023GL105064.

[69] H. de Moel, J.C.J.H. Aerts, Effect of uncertainty in land use, damage models and inundation depth on flood damage estimates, Nat. Haz. 58 (2011) 407-425. https://doi.org/10.1007/s11069-010-9675-6.

[70] S. Dasgupta, M. Huq, Z.H. Khan, M.M.Z. Ahmed, N. Mukherjee, M.F. Khan, K. Pandey Vulnerability of Bangladesh to cyclones in a changing climate potential damages and adaptation cost, Policy Res. Working Paper (2010) 5280 . https://ssrn.com/abstract=1596490.

[71] B. Ntanganedzeni, J. Nobert, Flood risk assessment in Luvuvhu river, Limpopo province, South Africa, Phys. Chem. Earth 124 (2021) 102959. https://doi.org/10.1016/j.pce.2020.102959.

[72] K. Komi, B.A. Amisigo, B. Diekkrüger, Integrated flood risk assessment of rural communities in the Oti River basin, West Africa, Hydrology 3 (2016) 42. https://doi.org/10.3390/hydrology3040042.

[73] C.D.Q. Alfonso, M.B. Sundo, R.G. Zafra, P.P. Velasco, J.J.C. Aguirre, M.S. Madlangbayan, Flood risk assessment of major river basins in the Philippines, Int. J. Geomate 17 (2019) 201–208. https://doi.org/10.21660/2019.64.17155.

[74] S. Mahmood, A. Rahman, R. Shaw, Spatial appraisal of flood risk assessment and evaluation using integrated hydro-probabilistic approach in Panjkora River Basin, Pakistan, Environ. Monit. Assess. 191 (2019) 573, https://doi.org/10.1007/s10661-019-7746-z.

[75] K. Mishra, R. Sinha, Flood risk assessment in the Kosi megafan using multi-criteria decision analysis: a hydro-geomorphic approach, Geomorph. 350 (2020) 106861. https://doi.org/10.1016/j.geomorph.2019.106861.

[76] S. Roy, A. Bose, I.R. Chowdhury, Flood risk assessment using geospatial data and multi-criteria decision approach: a study from historically active flood-prone region of Himalayan foothill, India, Arabian J. Geosci. 14 (2021) 999. https://doi.org/10.1007/s12517-021-07324-8.

[77] A. Shuaibu, J. Hounkpè, Y.A. Bossa, R.M. Kalin, Flood risk assessment and mapping in the Hadejia River basin, Nigeria, using hydro-geomorphic approach and multi-criterion decision-making method, Water (2022) 14, 3709. https://doi.org/10.3390/w14223709.

[78] E. Mokhtari, F. Mezali, B. Abdelkebir, B. Engel, Flood risk assessment using analytical hierarchy process: A case study from the Cheliff-Ghrib watershed, Algeria, J. Water Clim. Chang. 14 (2023) 694. https://doi.org/10.2166/wxx.2023.316.

[79] O.O. Aladejana, E.J. Ebijuoworih, Flood risk assessment in Kogi State Nigeria through the integration of hazard and vulnerability factors, Discover Geosci. 2 (2024) 31. https://doi.org/10.1007/s44288-024-00036-y.

[80] Y.A. Bossa, O. Djangni, Y. Yira, J. Hounkpè, A.D. Avossè, L.O. Sintondji, Flood risk assessment in the lower valley of Ouémé, Benin, Open J. Modern Hydrol. 14 (2024) 130–151. https://www.scirp.org/journal/ojmh.

[81] H.D. Nguyen, T.H.T. Nguyen, Q.-H. Nguyen, T.G. Nguyen, D.K. Dang, Y.N. Nguyen, T.H. Bui, N.D. Nguyen, Q.-T. Bui, P. Brecan, A.I. Petrisor, Bottom-up approach for flood-risk management in developing countries: a case study in the Gianh River watershed of Vietnam, Nat. Haz. 118 (2023) 1933–1959. https://doi.org/10.1007/s11069-023-06098-4.

[82] Z. Brahim, R. Boualemb, M. Azzeddine, Flood risk assessment using modern models integrated with GIS for susceptibility mapping of the M'zab Valley watershed (Algeria), Water Sci. Tech. 90 (2024) 2352. https://doi.org/10.2166/wst.2024.343.

[83] P. Syldon, B.B. Shrestha, M. Miyamoto, K. Tamakawa, S. Nakamura, 2024. Assessing the impact of climate change on flood inundation and agriculture in the Himalayan mountainous region of Bhutan, J. Hydro. Reg. Sci. 52, 101687. https://doi.org/10.1016/j.ejrh.2024.101687.

[84] N.A. Khan, H. Alzahrani, S. Bai, M. Hussain, M. Tayyab, S. Ullah, K. Ullah, S. Khalid, Flood risk assessment in the Swat river catchment through GIS-based multi-criteria decision analysis, Front. Environ. Sci. 13 (2025) 1567796. https://doi.org/10.3389/fenvs.2025.1567796.

[85] N.E.H. Belazreg, M. Hasbaia, Z. Şen, A. Ferhati, Flood risk mapping using multi-criteria analysis (MCA) through AHP method case of El-Ham wadi watershed of Hodna basin (Algeria), Nat. Haz. 120 (2024) 1023–1039. https://doi.org/10.1007/s11069-023-06239-9.

[86] I. Besarra, A. Opdyke, J.E. Mendoza, P.A. Delmendo, J. Santiago, D.J. Evangelista, A.M.F.A. Lagmay, The cost of flooding on housing under climate change in the Philippines: examining projected damage at the local scale, J. Environ. Manag. 380 (2025) 124966. https://doi.org/10.1016/j.jenvman.2025.124966.

[87] F. Gholami, Y. Li, J. Zhang, A. Nemati, Quantitative assessment of future environmental changes in hydrological risk components: integration of remote sensing, machine learning, and hydraulic modelling, Water. 16 (2024) 3354. https://doi.org/10.3390/w16233354.

[88] A.E. Piggott-McKellar, J. Pearson, K.E. McNamara, P.D. Nunn, A livelihood analysis of resettlement outcomes: Lessons for climate-induced relocations, Ambio 49 (2020) 1474–1489. https://doi.org/10.1007/s13280-019-01289-5.

Journal Pre-proof

Journal Pre-proof

Integrating high-resolution geoinformation with local knowledge enhances flood risk assessment: A case study from rural Niger

Highlights

File: Highlights_5.6.2026
386 words, 388 characters

- River flooding during the dry season causes more damage than during the wet season
- Expected damage to irrigated crops is greater than damage to buildings
- High-resolution geoinformation and local knowledge identify feasible risk reduction
- Raising the embankments, early warning, hygiene and sanitation are priorities
- High land prices hinder resettlement and redirect land development

Journal Pre-proof

Journal Pre-proof

Declaration of interests

☐ The authors declare that they have no known competing financial interests or personal relationships that could have appeared to influence the work reported in this paper.

☒ The authors declare the following financial interests/personal relationships which may be considered as potential competing interests:

Maurizio Tiepolo reports financial support was provided by Italian Agency for Development Cooperation. If there are other authors, they declare that they have no known competing financial interests or personal relationships that could have appeared to influence the work reported in this paper.

Journal Pre-proof